

## Mean-square convergence of the BDF2-Maruyama and backward Euler schemes for SDE satisfying a global monotonicity condition

Adam Andersson · Raphael Kruse

Received: date / Accepted: date

**Abstract** In this paper the numerical approximation of stochastic differential equations satisfying a global monotonicity condition is studied. The strong rate of convergence with respect to the mean square norm is determined to be  $\frac{1}{2}$  for the two-step BDF-Maruyama scheme and for the backward Euler-Maruyama method. In particular, this is the first paper which proves a strong convergence rate for a multi-step method applied to equations with possibly superlinearly growing drift and diffusion coefficient functions. We also present numerical experiments for the  $\frac{3}{2}$ -volatility model from finance and a two dimensional problem related to Galerkin approximation of SPDE, which verify our results in practice and indicate that the BDF2-Maruyama method offers advantages over Euler-type methods if the stochastic differential equation is stiff or driven by a noise with small intensity.

**Keywords** SODE · backward Euler-Maruyama method · BDF2-Maruyama method · strong convergence rates · global monotonicity condition

**Mathematics Subject Classification (2010)** 65C30 · 65L06 · 65L20

---

Adam Andersson  
Technische Universität Berlin  
Institut für Mathematik, Secr. MA 5-3  
Straße des 17. Juni 136  
DE-10623 Berlin  
Germany  
Tel.: +49 (0) 30 314 - 2 96 80  
Fax: +49 (0) 30 314 - 2 89 67  
E-mail: andersson@math.tu-berlin.de

Raphael Kruse  
Technische Universität Berlin  
Institut für Mathematik, Secr. MA 5-3  
Straße des 17. Juni 136  
DE-10623 Berlin  
Germany  
Tel.: +49 (0) 30 314 - 2 33 54  
Fax: +49 (0) 30 314 - 2 89 67  
E-mail: kruse@math.tu-berlin.de

## 1 Introduction

Strong convergence rates of numerical approximations to stochastic differential equations (SDEs) are a well studied topic. Under a global Lipschitz condition on the coefficients the picture is rather complete, both for one-step methods [13], [17] and multi-step methods [2], [14]. Many important equations in application have coefficients that do not satisfy the global Lipschitz condition, and it is therefore important to study a more general setting. Many convergence results for explicit and implicit one-step methods have also been proven for equations without the global Lipschitz condition, see for instance [1], [7], [8], [9], [10], [12], [16], [19], [21]. In the present paper we determine the strong rate  $\frac{1}{2}$  for the backward Euler-Maruyama method (BEM), in the mean-square norm, which improves [16] in terms of a weaker assumption on the coefficients.

For multi-step schemes, on the other hand, there are no previously known results on strong convergence for equations with coefficients not satisfying a global Lipschitz condition. In this paper we determine the strong rate  $\frac{1}{2}$  for the BDF2-Maruyama scheme for equations whose, possibly superlinearly growing, coefficient functions satisfy a global monotonicity condition. Backward difference formulas (BDF) are popular in applied sciences for the approximation of stiff equations, see [2] for a list of references to such works.

Let  $d, m \in \mathbf{N}$ ,  $T > 0$  and  $(\Omega, \mathcal{F}, (\mathcal{F}_t)_{t \in [0, T]}, \mathbf{P})$  be a filtered probability space satisfying the usual conditions, on which an  $\mathbf{R}^d$ -valued standard  $(\mathcal{F}_t)_{t \in [0, T]}$ -Wiener process  $W : [0, T] \times \Omega \rightarrow \mathbf{R}^d$  is defined. We consider the equation

$$X(t) = X_0 + \int_0^t f(X(s)) ds + \int_0^t g(X(s)) dW(s), \quad t \in [0, T], \quad (1.1)$$

with drift  $f : \mathbf{R}^m \rightarrow \mathbf{R}^m$  and diffusion coefficient function  $g : \mathbf{R}^m \rightarrow \mathbf{R}^{m \times d}$ . The functions  $f$  and  $g$  are assumed to satisfy a global monotonicity, a coercivity and a local Lipschitz condition in Assumption 2.1 below. The initial condition fulfills  $X_0 \in L^2(\Omega, \mathcal{F}_0, \mathbf{P}; \mathbf{R}^m)$  with some additional integrability, admitting higher moments of the solution.

For a given equidistant time step size  $h \in (0, 1)$  we discretize the exact solution to (1.1) along the temporal grid  $\tau_h = \{t_n = nh : n = 0, 1, \dots, N_h\}$ . Here  $N_h \in \mathbf{N}$  is uniquely determined by the inequality  $t_{N_h} \leq T < t_{N_h+1}$ . We set  $\Delta_h W^j := W(t_j) - W(t_{j-1})$  for  $j \in \{1, \dots, N_h\}$ . We consider discretizations by means of the *backward Euler-Maruyama method*

$$X_h^j - X_h^{j-1} = hf(X_h^j) + g(X_h^{j-1})\Delta_h W^j, \quad j \in \{1, \dots, N_h\}, \quad (1.2)$$

with  $(X_h^0)_{h \in (0, 1)}$  satisfying  $\mathbf{E}[||X_h^0 - X_0||^2] = \mathcal{O}(h)$ , and by means of the *BDF2-Maruyama scheme* from [2]. The latter is given by the recursion

$$\frac{3}{2}X_h^j - 2X_h^{j-1} + \frac{1}{2}X_h^{j-2} = hf(X_h^j) + \frac{3}{2}g(X_h^{j-1})\Delta_h W^j - \frac{1}{2}g(X_h^{j-2})\Delta_h W^{j-1}, \quad (1.3)$$

for  $j \in \{2, \dots, N_h\}$ , with initial values  $(X_h^0, X_h^1)$  where  $(X_h^0)_{h \in (0, 1)}$  is the same as above and  $(X_h^1)_{h \in (0, 1)}$  is determined, for instance, by one step of the backward Euler scheme

or some other one-step method satisfying  $\mathbf{E}[\|X_h^1 - X(h)\|^2] = \mathcal{O}(h)$ . In practice, the implementation of the methods (1.2) and (1.3) often requires to solve a nonlinear equation in each time step. In Section 3 we discuss that under our assumptions a solution does indeed always exist provided the step size  $h$  is small enough. The choice of the root-finding algorithm may depend on the coefficient function  $f$  and its smoothness. We refer to [18] for a collection of such methods.

We prove that for  $(X_h^j)_{j \in \{0, \dots, N_h\}, h \in (0, 1)}$ , determined either by (1.2) or (1.3), and  $X$  being the solution to (1.1), there exist a constant  $C$  such that the following mean-square convergence holds:

$$\max_{j \in \{0, \dots, N_h\}} \|X(t_j) - X_h^j\|_{L^2(\Omega; \mathbf{R}^m)} \leq C\sqrt{h}, \quad h \in (0, 1). \quad (1.4)$$

The precise statements of our convergence results are found in Theorems 4.4 and 5.4. The proofs are based on two elementary identities: for all  $u_1, u_2 \in \mathbf{R}^m$  it holds that

$$2(u_2 - u_1, u_2) = |u_2|^2 - |u_1|^2 + |u_2 - u_1|^2, \quad (1.5)$$

and for all  $u_1, u_2, u_3 \in \mathbf{R}^m$  it holds that

$$\begin{aligned} & 4\left(\frac{3}{2}u_3 - 2u_2 + \frac{1}{2}u_1, u_3\right) \\ &= |u_3|^2 - |u_2|^2 + |2u_3 - u_2|^2 - |2u_2 - u_1|^2 + |u_3 - 2u_2 + u_1|^2, \end{aligned} \quad (1.6)$$

found in [3], which has been derived from results on  $G$ -stability for linear multi-step methods, see [4, 20]. Up to the best of our knowledge (1.6) has not previously been used in the study of the BDF2 scheme for stochastic differential equations.

The paper is organized as follows: Section 2 contains notation and our precise assumptions on the coefficients  $f$  and  $g$  in (1.1). We cite well known results on existence, uniqueness and moment bounds for the solution under these conditions. A well-posedness result for general implicit stochastic difference equations is proved in Section 3. Sections 4 and 5 contain the analysis of the backward Euler-Maruyama and the BDF2-Maruyama schemes, respectively. Subsections 4.1 and 5.1 contain a priori estimates for the respective schemes, in Sections 4.2 and 5.2 stability results are proved, while Subsections 4.3 and 5.3 are concerned with the consistency of the two schemes. The two main results on the strong mean-square convergence rate are stated in Sections 4.4 and 5.4, respectively. Further, in Subsection 5.5 we have a closer look on the second initial value for the BDF2-Maruyama scheme and it is shown that using one step of the BEM method is a feasible choice. Section 6 contains numerical experiments involving the  $\frac{3}{2}$ -volatility model from finance which verify our theoretical results and indicate that the BDF2-Maruyama method performs better than Euler-type methods in case of stiff problems or equations with a small noise intensity.

## 2 Setting and preliminaries

### 2.1 Notation and function spaces

Let  $(\cdot, \cdot)$  and  $|\cdot|$  denote the scalar product and norm in  $\mathbf{R}^m$  and let  $|\cdot|_{\text{HS}}$  denote the Hilbert-Schmidt norm on the space  $\mathbf{R}^{m \times d}$  of all  $m$  times  $d$  matrices, i.e.,  $|S|_{\text{HS}} = \sqrt{\text{Tr}(S^*S)}$  for  $S \in \mathbf{R}^{m \times d}$ .

Let  $(\Omega, \mathcal{F}, (\mathcal{F}_t)_{t \in [0, T]}, \mathbf{P})$  be a filtered probability space satisfying the usual conditions. For  $p \in [1, \infty)$  and a sub- $\sigma$ -field  $\mathcal{G} \subset \mathcal{F}$  we denote by  $L^p(\Omega, \mathcal{G}, \mathbf{P}; E)$  the Banach space of all  $p$ -fold integrable,  $\mathcal{G}/\mathcal{B}(E)$ -measurable random variables taking values in a Banach space  $(E, |\cdot|_E)$  with norm

$$\|Z\|_{L^p(\Omega, \mathcal{G}, \mathbf{P}; E)} = (\mathbf{E}[|Z|_E^p])^{\frac{1}{p}}, \quad Z \in L^p(\Omega, \mathcal{G}, \mathbf{P}; E).$$

If  $\mathcal{G} = \mathcal{F}$  we write  $L^p(\Omega; E) := L^p(\Omega, \mathcal{F}, \mathbf{P}; E)$ . If  $p = 2$  and  $E = \mathbf{R}^m$  we obtain the Hilbert space  $L^2(\Omega; \mathbf{R}^m)$  with inner product and norm

$$\langle X, Y \rangle = \mathbf{E}[\langle X, Y \rangle], \quad \|X\| = \sqrt{\langle X, X \rangle},$$

for all  $X, Y \in L^2(\Omega; \mathbf{R}^m)$ . We denote by  $\| \cdot \|$  the norm in  $L^2(\Omega; \mathbf{R}^{m \times d})$ , i.e.,  $\|Z\| = (\mathbf{E}[|Z|_{\text{HS}}^2])^{\frac{1}{2}}$  for  $Z \in L^2(\Omega; \mathbf{R}^{m \times d})$ .

We next introduce notation related to the numerical discretizations. Recall from Section 1 the temporal grids  $\tau_h$ ,  $h \in (0, 1)$ . For  $h \in (0, 1)$  and  $j \in \{0, \dots, N_h\}$ , we denote by

$$P_h^j : L^2(\Omega, \mathcal{F}, \mathbf{P}; \mathbf{R}^m) \rightarrow L^2(\Omega, \mathcal{F}_{t_j}, \mathbf{P}; \mathbf{R}^m),$$

the orthogonal projector onto the closed sub-space  $L^2(\Omega, \mathcal{F}_{t_j}, \mathbf{P}; \mathbf{R}^m)$ , which is also known as the conditional expectation. More precisely, for  $Y \in L^2(\Omega; \mathbf{R}^m)$  we set  $P_h^j Y = \mathbf{E}[Y | \mathcal{F}_{t_j}]$ . We introduce the spaces  $(\mathcal{G}_h^2)_{h \in (0, 1)}$  of all adapted grid functions, which enjoy the following integrability properties

$$\begin{aligned} \mathcal{G}_h^2 := \{ & Z : \{0, \dots, N_h\} \times \Omega \rightarrow \mathbf{R}^m : Z^n, f(Z^n) \in L^2(\Omega, \mathcal{F}_{t_n}, \mathbf{P}; \mathbf{R}^m), \\ & g(Z^n) \in L^2(\Omega, \mathcal{F}_{t_n}, \mathbf{P}; \mathbf{R}^{m \times d}) \text{ for } n \in \{0, \dots, N_h\} \}. \end{aligned}$$

These will play an important role in the error analysis.

### 2.2 Setting

Consider the setting introduced in Section 1. We now formulate our assumptions on the initial condition and the coefficient functions  $f$  and  $g$  which we work with throughout this paper.

**Assumption 2.1** There exists  $q \in [1, \infty)$  such that the initial condition  $X_0 : \Omega \rightarrow \mathbf{R}^m$  satisfies  $X_0 \in L^{4q-2}(\Omega, \mathcal{F}_0, \mathbf{P}; \mathbf{R}^m)$ . Moreover, the mappings  $f : \mathbf{R}^m \rightarrow \mathbf{R}^m$  and

$g: \mathbf{R}^m \rightarrow \mathbf{R}^{m \times d}$ , are continuous and there exist  $L \in (0, \infty)$  and  $\eta \in (\frac{1}{2}, \infty)$  such that for all  $x_1, x_2 \in \mathbf{R}^m$  it holds

$$(f(x_1) - f(x_2), x_1 - x_2) + \eta |g(x_1) - g(x_2)|_{\text{HS}}^2 \leq L|x_1 - x_2|^2, \quad (2.1)$$

$$|f(x_1) - f(x_2)| \leq L(1 + |x_1|^{q-1} + |x_2|^{q-1})|x_1 - x_2|, \quad (2.2)$$

where  $q \in [1, \infty)$  is the same as above. Further, it holds for all  $x \in \mathbf{R}^m$  that

$$(f(x), x) + \frac{4q-3}{2} |g(x)|_{\text{HS}}^2 \leq L(1 + |x|^2). \quad (2.3)$$

Assumption 2.1 guarantees the existence of an up to modification unique adapted solution  $X: [0, T] \times \Omega \rightarrow \mathbf{R}^m$  to (1.1) with continuous sample paths, satisfying

$$\sup_{t \in [0, T]} \|X(t)\|_{L^{4q-2}(\Omega; \mathbf{R}^m)} < \infty, \quad (2.4)$$

see, e.g., [15, Chap. 2]. In the proof of Theorem 5.3 on the consistency of the BDF2 scheme, the  $L^{4q-2}(\Omega; \mathbf{R}^m)$ -moment bound is of importance in order to apply the bounds (4.5), (4.6) below.

For later reference we note several consequences of Assumption 2.1. From (2.2) we deduce the following polynomial growth bound:

$$|f(x)| \leq \tilde{L}(1 + |x|^q), \quad x \in \mathbf{R}^m, \quad (2.5)$$

where  $\tilde{L} = 2L + |f(0)|$ . Indeed, (2.2) implies that

$$\begin{aligned} |f(x)| &\leq |f(x) - f(0)| + |f(0)| \leq L(1 + |x|^{q-1})|x| + |f(0)| \\ &\leq (2L + |f(0)|)(1 + |x|^q), \quad x \in \mathbf{R}^m. \end{aligned}$$

Moreover, from (2.1) followed by a use of (2.2) it holds, for  $x_1, x_2 \in \mathbf{R}^m$ , that

$$\begin{aligned} |g(x_1) - g(x_2)|_{\text{HS}}^2 &\leq \frac{L}{\eta} |x_1 - x_2|^2 + \frac{1}{\eta} |(f(x_1) - f(x_2), x_1 - x_2)| \\ &\leq \frac{L}{\eta} (2 + |x_1|^{q-1} + |x_2|^{q-1}) |x_1 - x_2|^2. \end{aligned}$$

This gives the local Lipschitz bound

$$|g(x_1) - g(x_2)|_{\text{HS}}^2 \leq \frac{2L}{\eta} (1 + |x_1|^{q-1} + |x_2|^{q-1}) |x_1 - x_2|^2, \quad x_1, x_2 \in \mathbf{R}^m, \quad (2.6)$$

and, in the same way as above, the polynomial growth bound

$$|g(x)|_{\text{HS}} \leq \bar{L}(1 + |x|^{\frac{q+1}{2}}), \quad x \in \mathbf{R}^m, \quad (2.7)$$

where  $\bar{L} = 2\sqrt{\frac{2L}{\eta}} + |g(0)|_{\text{HS}}$ . Finally, we note for later use that the restriction  $X|_{\tau_h}$  of the exact solution to the time grid  $\tau_h$ , given by

$$[X|_{\tau_h}]^j := X(jh), \quad j \in \{0, \dots, N_h\},$$

is an element of the space  $\mathcal{G}_h^2$  for every  $h \in (0, 1)$ . This follows directly from (2.4) and the growth bounds (2.5) and (2.7).

### 2.3 Preliminaries

Here we list some basic results that we use in this paper. Frequently, we apply the Young inequality and the weighted Young inequality

$$ab \leq \frac{a^2}{2} + \frac{b^2}{2} \quad \text{and} \quad ab \leq \frac{\nu}{2}a^2 + \frac{1}{2\nu}b^2, \quad (2.8)$$

which holds true for all  $a, b \in \mathbf{R}$  and  $\nu > 0$ . We make use of the following discrete version of Gronwall's Lemma: If  $h > 0$ ,  $a_1, \dots, a_{N_h}, b, c \in [0, \infty)$ , then

$$\forall n \in \{1, \dots, N_h\} : a_n \leq c + bh \sum_{j=1}^{n-1} a_j \quad \text{implies} \quad \forall n \in \{1, \dots, N_h\} : a_n \leq ce^{bt_n}. \quad (2.9)$$

Finally we cite a standard result from nonlinear analysis which we use for the well-posedness of the numerical schemes, see for instance [18, Chap. 6.4] or [20, Thm. C.2]:

**Proposition 2.1** *Let  $G: \mathbf{R}^m \rightarrow \mathbf{R}^m$  be a continuous mapping satisfying for some  $c \in (0, \infty)$*

$$(G(x_1) - G(x_2), x_1 - x_2) \geq c|x_1 - x_2|^2, \quad x_1, x_2 \in \mathbf{R}^m.$$

*Then  $G$  is a homeomorphism with Lipschitz continuous inverse. In particular, it holds*

$$|G^{-1}(y_1) - G^{-1}(y_2)| \leq \frac{1}{c}|y_1 - y_2|$$

*for all  $y_1, y_2 \in \mathbf{R}^m$ .*

### 3 A well-posedness result for stochastic difference equations

In this section we prove existence and uniqueness of solutions to general stochastic  $k$ -step difference equations. This result applies in particular to all implicit linear multi-step schemes for SDE with coefficients satisfying Assumption 2.1 including the backward Euler-Maruyama method, the Crank-Nicolson scheme, the  $k$ -step BDF-schemes, and the  $k$ -step Adams-Moulton methods. We refer the reader to [2, 14] for a thorough treatment of these schemes for stochastic differential equations with Lipschitz continuous coefficients.

**Theorem 3.1** *Let the mappings  $f$  and  $g$  satisfy Assumption 2.1 with  $q \in [1, \infty)$  and  $L \in (0, \infty)$ , let  $k \in \mathbf{N}$ ,  $\alpha_0, \dots, \alpha_{k-1}, \beta_0, \dots, \beta_{k-1}, \gamma_0, \dots, \gamma_{k-1} \in \mathbf{R}$ ,  $\alpha_k = 1$ ,  $\beta_k \in (0, \infty)$ , and  $h_1 \in (0, \frac{1}{\beta_k L})$  with  $kh_1 < T$ . Assume that initial values  $U_h^\ell \in L^2(\Omega, \mathcal{F}_{t_\ell}, \mathbf{P}; \mathbf{R}^m)$  are given with  $f(U_h^\ell) \in L^2(\Omega, \mathcal{F}_{t_\ell}, \mathbf{P}; \mathbf{R}^m)$  and  $g(U_h^\ell) \in L^2(\Omega, \mathcal{F}_{t_\ell}, \mathbf{P}; \mathbf{R}^{m \times d})$  for all  $\ell \in \{0, \dots, k-1\}$ . Then, for every  $h \in (0, h_1]$  there exists a unique family of adapted random variables  $U_h \in \mathcal{G}_h^2$  satisfying*

$$\sum_{\ell=0}^k \alpha_{k-\ell} U_h^{j-\ell} = h \sum_{\ell=0}^k \beta_{k-\ell} f(U_h^{j-\ell}) + \sum_{\ell=1}^k \gamma_{k-\ell} g(U_h^{j-\ell}) \Delta_h W^{j-\ell+1}, \quad (3.1)$$

for  $j \in \{k, \dots, N_h\}$ . In particular, it holds true that  $U_h^j, f(U_h^j) \in L^2(\Omega, \mathcal{F}_{t_j}, \mathbf{P}; \mathbf{R}^m)$  and  $g(U_h^j) \in L^2(\Omega, \mathcal{F}_{t_j}, \mathbf{P}; \mathbf{R}^{m \times d})$  for all  $j \in \{k, \dots, N_h\}$ .

*Proof* Let  $F_h: \mathbf{R}^m \rightarrow \mathbf{R}^m$ ,  $h \in (0, h_1]$ , be the mappings defined by

$$F_h(x) := x - h\beta_k f(x), \quad x \in \mathbf{R}^m; \quad h \in (0, h_1].$$

Note that for every  $h \in (0, h_1]$  it holds that  $1 - \beta_k h L \geq 1 - \beta_k h_1 L > 0$  and from the global monotonicity condition (2.1) we have that

$$\begin{aligned} (F_h(x_1) - F_h(x_2), x_1 - x_2) &= |x_1 - x_2|^2 - \beta_k h (f(x_1) - f(x_2), x_1 - x_2) \\ &\geq (1 - \beta_k h_1 L) |x_1 - x_2|^2. \end{aligned}$$

Consequently, by Proposition 2.1 the inverse  $F_h^{-1}$  of  $F_h$  exists for every  $h \in (0, h_1]$  and is globally Lipschitz continuous with Lipschitz constant  $(1 - h_1 \beta L)^{-1}$ . Using these properties and the fact that  $\alpha_k = 1$  we can rewrite (3.1) as

$$F_h(U_h^j) = R_h^j \iff U_h^j = F_h^{-1}(R_h^j) \quad (3.2)$$

for all  $j \in \{k, \dots, N_h\}$ , where

$$R_h^j := - \sum_{\ell=1}^k \alpha_{k-\ell} U_h^{j-\ell} + h \sum_{\ell=1}^k \beta_{k-\ell} f(U_h^{j-\ell}) + \sum_{\ell=1}^k \gamma_{k-\ell} g(U_h^{j-\ell}) \Delta_h W^{j-\ell+1},$$

for  $j \in \{k, \dots, N_h\}$ . Therefore, by (3.2) and the continuity of  $F_h^{-1}$  we have that for every  $h \in (0, h_1]$ ,  $U_h$  is an adapted collection of random variables, uniquely determined by the initial values  $U_h^0, \dots, U_h^{k-1}$ .

In order to prove that  $U_h \in \mathcal{G}_h^2$  for all  $h \in (0, h_1]$ , by means of an induction argument, we introduce  $U_h^{j,n} := U_h^j \mathbf{1}_{\{0, \dots, n-1\}}(j)$ . By the assumptions on the initial values  $U_h^0, \dots, U_h^{k-1}$  it holds that  $(U_h^{j,k})_{j \in \{0, \dots, N_h\}} \in \mathcal{G}_h^2$ . For the induction step, we now assume that  $(U_h^{j,n})_{j \in \{0, \dots, N_h\}} \in \mathcal{G}_h^2$  for some  $n \in \{k, \dots, N_h\}$ . This assumption and the fact that

$$\|g(U_h^{j-\ell}) \Delta_h W^{j-\ell+1}\|^2 = h \|g(U_h^{j-\ell})\|^2,$$

imply immediately that  $R_h^n \in L^2(\Omega, \mathcal{F}_{t_n}, \mathbf{P}; \mathbf{R}^m)$ . Thus, from the linear growth of  $F_h^{-1}$  we get  $U_h^n = F_h^{-1}(R_h^n) \in L^2(\Omega, \mathcal{F}_{t_n}, \mathbf{P}; \mathbf{R}^m)$ .

In addition, we recall from [1, Cor. 4.2] the fact that under Assumption 2.1 the mapping  $h^{\frac{1}{2}} g \circ F_h^{-1}$  is also globally Lipschitz continuous with a Lipschitz constant independent of  $h$ . More precisely, there exists a constant  $C$  such that for all  $h \in (0, h_1]$  and all  $x_1, x_2 \in \mathbf{R}^m$  it holds true that

$$h |g(F_h^{-1}(x_1)) - g(F_h^{-1}(x_2))|_{\text{HS}}^2 \leq C |x_1 - x_2|^2. \quad (3.3)$$

Consequently, the mapping  $h^{\frac{1}{2}} g \circ F_h^{-1}: \mathbf{R}^m \rightarrow \mathbf{R}^m$  is also of linear growth and we conclude as above

$$\|g(U_h^n) \Delta_h W^{n+1}\|^2 = h \|g(U_h^n)\|^2 = h \|g(F_h^{-1}(R_h^n))\|^2 \leq C(1 + \|R_h^n\|^2).$$

In particular, this gives  $g(U_h^n) \in L^2(\Omega, \mathcal{F}_n, \mathbf{P}; \mathbf{R}^{m \times d})$ . Finally, from the definition of  $F_h$  and (3.2) we have that

$$f(U_h^n) = \frac{1}{\beta_k h} (U_h^n + \beta_k h f(U_h^n) - U_h^n) = \frac{1}{\beta_k h} (U_h^n - F_h(U_h^n)) = \frac{1}{\beta_k h} (F_h^{-1}(R_h^n) - R_h^n).$$

Hence, by the linear growth of  $F_h^{-1}$  and the fact that  $R_h^n \in L^2(\Omega, \mathcal{F}_n, \mathbf{P}; \mathbf{R}^m)$  we conclude that  $f(U_h^n) \in L^2(\Omega, \mathcal{F}_n, \mathbf{P}; \mathbf{R}^m)$ .

Altogether, this proves that  $(U_h^{j,n+1})_{j \in \{0, \dots, N_h\}} \in \mathcal{G}_h^2$  and, therefore, by induction  $(U_h^{j,n})_{j \in \{0, \dots, N_h\}} \in \mathcal{G}_h^2$  for every  $n \in \{k, \dots, N_h + 1\}$ . By finally noting that  $U_h^j = U_h^{j, N_h+1}$ ,  $j \in \{0, \dots, N_h\}$ , the proof is complete.  $\square$

## 4 The backward Euler-Maruyama method

In this section we prove that the backward Euler-Maruyama scheme is mean-square convergent of order  $\frac{1}{2}$  under Assumption 2.1. The proof is split over several subsections: First we familiarize ourselves with the connection between the BEM method and the identity (1.5). This is done by proving an a priori estimate in Subsection 4.1. In Subsection 4.2 we then derive a stability result which gives an estimate of the distance between an arbitrary adapted grid function and the one generated by the BEM method. As it turns out this distance is bounded by the error in the initial value and a local truncation error. The latter is estimated for the restriction of the exact solution to (1.1) to the temporal grid  $\tau_h$  in Subsection 4.3. Altogether, this will then yield the desired convergence result in Section 4.4.

### 4.1 Basic properties of the backward Euler-Maruyama scheme

Here and in Subsection 4.2 we study  $U \in \mathcal{G}_h^2$ ,  $h \in (0, \frac{1}{L})$ , satisfying

$$U^j = U^{j-1} + hf(U^j) + g(U^{j-1})\Delta_h W^j, \quad j \in \{1, \dots, N_h\}, \quad (4.1)$$

with initial condition  $U^0 \in L^2(\Omega, \mathcal{F}_0, \mathbf{P}; \mathbf{R}^m)$  such that  $f(U^0) \in L^2(\Omega, \mathcal{F}_0, \mathbf{P}; \mathbf{R}^m)$  and  $g(U^0) \in L^2(\Omega, \mathcal{F}_0, \mathbf{P}; \mathbf{R}^{m \times d})$ . Here  $L$  is the parameter in Assumption 2.1 and from Theorem 3.1 there exist for every  $h \in (0, \frac{1}{L})$  a unique  $U \in \mathcal{G}_h^2$  satisfying (4.1).  $U_0$  is not necessarily related to the initial value  $X_0$  of (1.1).

In order to prove the a priori bound of Theorem 4.1 and the stability in Theorem 4.2 the following lemma is used:

**Lemma 4.1** *For all  $h \in (0, \frac{1}{L})$  and  $U, V \in \mathcal{G}_h^2$  with  $U$  satisfying (4.1) it holds for all  $j \in \{1, \dots, N_h\}$   $\mathbf{P}$ -almost surely that*

$$\begin{aligned} & |E^j|^2 - |E^{j-1}|^2 + |E^j - E^{j-1}|^2 \\ &= 2h(f(U^j), E^j) + 2(g(U^{j-1})\Delta_h W^j, E^j - E^{j-1}) - 2(V^j - V^{j-1}, E^j) + Z^j, \end{aligned}$$

where  $E := U - V$  and  $(Z^j)_{j \in \{1, \dots, N_h\}}$  are the centered random variables given by

$$Z^j := 2(g(U^{j-1})\Delta_h W^j, E^{j-1}).$$

*Proof* From the identity (1.5), and since  $U$  satisfies (4.1) by assumption the assertion follows directly. Note that  $Z^j$  is well-defined as a centered real-valued integrable random variable due to the independence of the centered Wiener increment  $\Delta_h W^j$  and the square integrable random variables  $g(U^{j-1})$  and  $E^{j-1}$ .  $\square$

The proof of the next theorem is the first and simplest demonstration of the, in principle, same technique used to prove Theorems 4.2, 5.1 and 5.2 below. This a priori estimate is in fact not needed further in the analysis and it can be deduced from the stability Theorem 4.2, but with larger constants, and for a more narrow range for the parameter  $h$ . We include it for completeness.

**Theorem 4.1** *Let Assumption 2.1 hold with  $L \in (0, \infty)$ ,  $q \in [1, \infty)$ . For  $h \in (0, \frac{1}{2L})$  denote by  $U \in \mathcal{G}_h^2$  the unique adapted grid function satisfying (4.1). Then, for all  $n \in \{1, \dots, N_h\}$  it holds that*

$$\|U^n\|^2 + h\|g(U^n)\|^2 \leq C_h \exp\left(\frac{2Lt_n}{1-2Lh}\right) \left(1 + \|U^0\|^2 + h\|g(U^0)\|^2\right),$$

where  $C_h = \max\{1, 2LT\}(1-2Lh)^{-1}$ .

*Proof* Lemma 4.1 applied with  $V = 0$  and taking expectations yields

$$\begin{aligned} & \|U^j\|^2 - \|U^{j-1}\|^2 + \|U^j - U^{j-1}\|^2 \\ &= 2h\langle f(U^j), U^j \rangle + 2\langle g(U^{j-1})\Delta_h W^j, U^j - U^{j-1} \rangle. \end{aligned}$$

From the coercivity condition (2.3) and the Young inequality (2.8) we have that

$$\|U^j\|^2 - \|U^{j-1}\|^2 \leq 2h\left(L(1 + \|U^j\|^2) - \frac{4q-3}{2}\|g(U^j)\|^2\right) + h\|g(U^{j-1})\|^2.$$

Summing over  $j$  from 1 to  $n$  gives that

$$\begin{aligned} & (1-2Lh)\|U^n\|^2 + (4q-3)h\|g(U^n)\|^2 \\ & \leq 2LT + \|U^0\|^2 + h\|g(U^0)\|^2 + (4-4q)h \sum_{j=1}^{n-1} \|g(U^j)\|^2 + 2Lh \sum_{j=1}^{n-1} \|U^j\|^2. \end{aligned}$$

Since  $q \in [1, \infty)$  it holds  $1 \leq 4q-3$  and  $4-4q \leq 0$ . By elementary bounds we get

$$\|U^n\|^2 + h\|g(U^n)\|^2 \leq \frac{2LT + \|U^0\|^2 + h\|g(U^0)\|^2}{1-2Lh} + \frac{2L}{1-2Lh}h \sum_{j=1}^{n-1} \|U^j\|^2.$$

We conclude by a use of the discrete Gronwall Lemma (2.9).  $\square$

## 4.2 Stability of the backward Euler-Maruyama scheme

For the formulation of the stability Theorem 4.2 we define for  $h \in (0, 1)$  and  $V \in \mathcal{G}_h^2$  the *local truncation error* of  $V$  given by

$$\rho_h^{\text{BEM}}(V) := \sum_{j=1}^{N_h} \|\rho_h^j(V)\|^2 + \frac{1}{h} \sum_{j=1}^{N_h} \|P_h^{j-1} \rho_h^j(V)\|^2, \quad (4.2)$$

where the *local residuals*  $\rho_h^j(V)$  of  $V$  are defined as

$$\rho_h^j(V) := hf(V^j) + g(V^{j-1})\Delta_h W^j - V^j + V^{j-1},$$

for  $j \in \{2, \dots, N_h\}$ . Note that  $\rho_h^j(V) \in L^2(\Omega, \mathcal{F}_{t_j}, \mathbf{P}; \mathbf{R}^m)$  for every  $V \in \mathcal{G}_h^2$ . We also introduce a maximal step size  $h_E$  for the stability, which guarantees that the stability constant in Theorem 4.2 does not depend on  $h$ . It is given by

$$h_E = \frac{1}{\max\{4L, 2\}}. \quad (4.3)$$

Using the same arguments as in Theorem 4.1 the assertion of Theorem 4.2 stays true for all  $h \in (0, \frac{1}{2L})$  but with a constant  $C$  depending on  $\frac{1}{1-2hL}$  as in Theorem 4.1.

**Theorem 4.2** *Let Assumption 2.1 hold with  $L \in (0, \infty)$ ,  $\eta \in (\frac{1}{2}, \infty)$ . For all  $h \in (0, h_E]$ ,  $U \in \mathcal{G}_h^2$  satisfying (4.1),  $V \in \mathcal{G}_h^2$ , and all  $n \in \{1, \dots, N_h\}$  it holds that*

$$\begin{aligned} & \|U^n - V^n\|^2 + h \|g(U^n) - g(V^n)\|^2 \\ & \leq C \exp(2(1+2L)t_n) \left( \|U^0 - V^0\|^2 + h \|g(U^0) - g(V^0)\|^2 + \rho_h^{\text{BEM}}(V) \right), \end{aligned}$$

where  $C = \max\{3, 4\eta, \frac{4\eta}{2\eta-1}\}$ .

*Proof* Fix arbitrary  $h \in (0, h_E]$  and  $V \in \mathcal{G}_h^2$ . To ease the notation we suppress the dependence of  $h$  and  $V$  and simply write, for instance,  $\Delta W^j := \Delta_h W^j$ . We also write  $E^j := U^j - V^j$  and

$$\Delta f^j := f(U^j) - f(V^j), \quad \Delta g^j := g(U^j) - g(V^j), \quad j \in \{0, \dots, N_h\}. \quad (4.4)$$

From Lemma 4.1 we get after taking expectations that

$$\begin{aligned} & \|E^j\|^2 - \|E^{j-1}\|^2 + \|E^j - E^{j-1}\|^2 \\ & = 2h \langle \Delta f^j, E^j \rangle + 2 \langle \Delta g^{j-1} \Delta W^j + \rho^j, E^j - E^{j-1} \rangle + 2 \langle \rho^j, E^{j-1} \rangle. \end{aligned}$$

In order to treat the residual term we first notice that  $P_h^{j-1} E^{j-1} = E^{j-1}$ . Then, by taking the adjoint of the projector and by applying the weighted Young inequality (2.8) with  $v = h > 0$  we obtain

$$2 \langle \rho^j, E^{j-1} \rangle = 2 \langle P_h^{j-1} \rho^j, E^{j-1} \rangle \leq \frac{1}{h} \|P_h^{j-1} \rho^j\|^2 + h \|E^{j-1}\|^2.$$

Moreover, further applications of the Cauchy-Schwarz inequality, the triangle inequality, and the weighted Young inequality (2.8) with  $v = \mu$  yield

$$\begin{aligned} & 2\langle \Delta g^{j-1} \Delta W^j + \rho^j, E^j - E^{j-1} \rangle \\ & \leq \|\Delta g^{j-1} \Delta W^j + \rho^j\|^2 + \|E^j - E^{j-1}\|^2 \\ & \leq (1 + \mu) \|\Delta g^{j-1} \Delta W^j\|^2 + \left(1 + \frac{1}{\mu}\right) \|\rho^j\|^2 + \|E^j - E^{j-1}\|^2. \end{aligned}$$

Therefore, together with the global monotonicity condition (2.1) this gives

$$\begin{aligned} \|E^j\|^2 - \|E^{j-1}\|^2 & \leq 2hL\|E^j\|^2 - 2h\eta\|\Delta g^j\|^2 + (1 + \mu)h\|\Delta g^{j-1}\|^2 \\ & \quad + h\|E^{j-1}\|^2 + \left(1 + \frac{1}{\mu}\right) \|\rho^j\|^2 + \frac{1}{h} \|P_h^{j-1} \rho^j\|^2. \end{aligned}$$

Setting  $\mu = 2\eta - 1 > 0$  gives that  $1 + \mu = 2\eta$ . Then, summing over  $j$  from 1 to  $n$  and thereby identifying two telescoping sums yields

$$\begin{aligned} & (1 - 2Lh)\|E^n\|^2 + 2\eta h\|\Delta g^n\|^2 \\ & \leq (1 + h)\|E^0\|^2 + 2\eta h\|\Delta g^0\|^2 + (1 + 2L)h \sum_{j=1}^{n-1} \|E^j\|^2 \\ & \quad + \frac{2\eta}{2\eta - 1} \sum_{j=1}^n \|\rho^j\|^2 + \frac{1}{h} \sum_{j=1}^n \|P_h^{j-1} \rho^j\|^2. \end{aligned}$$

Since  $1 - 2Lh \geq 1 - 2Lh_E > \frac{1}{2}$  as well as  $h \leq h_E < \frac{1}{2}$  and  $\eta > \frac{1}{2}$  we obtain after some elementary transformations the inequality

$$\begin{aligned} \|E^n\|^2 + h\|\Delta g^n\|^2 & \leq \max\left\{3, 4\eta, \frac{4\eta}{2\eta - 1}\right\} \left(\|E^0\|^2 + h\|\Delta g^0\|^2 + \rho_h^{\text{BEM}}(V)\right) \\ & \quad + 2(1 + 2L)h \sum_{j=1}^{n-1} \|E^j\|^2. \end{aligned}$$

The proof is completed by applying the discrete Gronwall Lemma (2.9).  $\square$

### 4.3 Consistency of the backward Euler-Maruyama scheme

In this subsection we give an estimate for the local truncation error (4.2) of the BEM method. For the proof we first recall that the restriction  $X|_{\tau_h}$  of the exact solution to the temporal grid  $\tau_h$  is an element of the space  $\mathcal{G}_h^2$ , see Subsection 2.2. Further, we make use of [1, Lemma 5.5, Lemma 5.6], which provide estimates for the drift integral

$$\int_{\tau_1}^{\tau_2} \|f(X(\tau)) - f(X(s))\| ds \leq C \left(1 + \sup_{t \in [0, T]} \|X(t)\|_{L^{4q-2}(\Omega; \mathbf{R}^m)}^{2q-1}\right) |\tau_2 - \tau_1|^{\frac{3}{2}}, \quad (4.5)$$

for all  $\tau, \tau_1, \tau_2 \in [0, T]$  with  $\tau_1 \leq \tau \leq \tau_2$ , and for the stochastic integral

$$\left\| \int_{\tau_1}^{\tau_2} (g(X(\tau_1)) - g(X(s))) dW(s) \right\| \leq C \left( 1 + \sup_{t \in [0, T]} \|X(t)\|_{L^{4q-2}(\Omega; \mathbf{R}^m)}^{2q-1} \right) |\tau_2 - \tau_1|, \quad (4.6)$$

for all  $\tau_1, \tau_2 \in [0, T]$  with  $\tau_1 \leq \tau_2$ , respectively.

**Theorem 4.3** *Let Assumption 2.1 hold and let  $X|_{\tau_h}$  be the restriction of the exact solution to (1.1) to the temporal grid  $\tau_h$ . Then there exists  $C > 0$  such that*

$$\rho_h^{\text{BEM}}(X|_{\tau_h}) \leq Ch, \quad h \in (0, 1),$$

where the local truncation is defined in (4.2).

*Proof* Recall the definitions of  $\rho_h^{\text{BEM}}(X|_{\tau_h})$  and  $\rho_h^j(X|_{\tau_h})$  from (4.2). It suffices to show

$$\max_{j \in \{1, \dots, N_h\}} \left( \|\rho_h^j(X|_{\tau_h})\|^2 + \frac{1}{h} \|P_h^{j-1} \rho_h^j(X|_{\tau_h})\|^2 \right) \leq Ch^2. \quad (4.7)$$

Inserting (1.1) it holds for every  $j \in \{1, \dots, N_h\}$  that

$$\begin{aligned} \rho_h^j(X|_{\tau_h}) &= \int_{t_{j-1}}^{t_j} (f(X(t_j)) - f(X(s))) ds \\ &\quad + \int_{t_{j-1}}^{t_j} (g(X(t_{j-1})) - g(X(s))) dW(s) \\ P_h^{j-1} \rho_h^j(X|_{\tau_h}) &= \mathbf{E} \left[ \int_{t_{j-1}}^{t_j} (f(X(t_j)) - f(X(s))) ds \middle| \mathcal{F}_{t_{j-1}} \right]. \end{aligned}$$

Note that inequalities (4.5) and (4.6) apply to (4.7) due to the moment bound (2.4). These estimates together with an application of the triangle inequality and the fact that  $\|\mathbf{E}[V | \mathcal{F}_{t_{j-1}}]\| \leq \|V\|$  for every  $V \in L^2(\Omega; \mathbf{R}^m)$  completes the proof of (4.7).  $\square$

#### 4.4 Mean-square convergence of the backward Euler-Maruyama method

Here we consider the numerical approximations  $(X_h^j)_{j=0}^{N_h}$ ,  $h \in (0, h_E]$ , uniquely determined by the backward Euler-Maruyama method (1.2) with a corresponding family of initial values  $(X_h^0)_{h \in (0, h_E]}$ . Recall from (4.3) that  $h_E = \frac{1}{2(4L+1)}$ . This family is assumed to satisfy the following assumption.

**Assumption 4.1** The family of initial values  $(X_h^0)_{h \in (0, h_E]}$  satisfies

$$X_h^0, f(X_h^0) \in L^2(\Omega, \mathcal{F}_0, \mathbf{P}; \mathbf{R}^m), \quad g(X_h^0) \in L^2(\Omega, \mathcal{F}_0, \mathbf{P}; \mathbf{R}^{m \times d}), \quad (4.8)$$

for all  $h \in (0, h_E]$  and is consistent of order  $\frac{1}{2}$  in the sense that

$$\|X(0) - X_h^0\|^2 + h \|g(X(0)) - g(X_h^0)\|^2 = \mathcal{O}(h), \quad (4.9)$$

as  $h \downarrow 0$ , where  $X$  is the exact solution to (1.1).

Note that Assumption 4.1 is obviously satisfied for the choice  $X_h^0 := X_0$  for every  $h \in (0, h_E]$ . This said we are now ready to state the main result of this section.

**Theorem 4.4** *Let Assumptions 2.1 and 4.1 hold, let  $X$  be the exact solution to (1.1) and let  $(X_h^j)_{j=0}^{N_h}$ ,  $h \in (0, h_E]$ , be the family of backward Euler-Maruyama approximations determined by (1.2) with initial values  $(X_h^0)_{h \in (0, h_E]}$ . Then, the backward Euler-Maruyama method is mean-square convergent of order  $\frac{1}{2}$ , more precisely, there exists  $C > 0$  such that*

$$\max_{n \in \{0, \dots, N_h\}} \|X_h^n - X(nh)\| \leq C\sqrt{h}, \quad h \in (0, h_E].$$

*Proof* For  $h \in (0, h_E]$ , we apply Theorem 4.2 with  $U = (X_h^j)_{j=0}^{N_h} \in \mathcal{G}_h^2$  and  $V = X|_{\tau_h} = (X(t_j))_{j=0}^{N_h} \in \mathcal{G}_h^2$  and get that there is a constant  $C > 0$ , not depending on  $h$ , such that

$$\|X_h^n - X(nh)\|^2 \leq C(\|X_h^0 - X(0)\|^2 + h\|g(X_h^0) - g(X(0))\|^2 + \rho_h^{\text{BEM}}(X|_{\tau_h})).$$

The first and second term on the right hand side are of order  $\mathcal{O}(h)$  by Assumption 4.1. Since the same holds true for the consistency term  $\rho_h^{\text{BEM}}(X|_{\tau_h})$  by Theorem 4.3 the proof is completed.  $\square$

## 5 The BDF2-Maruyama method

In this section we follow the same procedure as in Section 4 with identity (1.6) in place of (1.5). Every result in Section 4 has its counterpart here for the BDF2-Maruyama method. As the multi-step method involves more terms the proofs in this section are naturally a bit more technical, but rely in principle on the same arguments as in the previous section.

### 5.1 Basic properties of the BDF2-Maruyama method

Here and in Subsection 5.2 our results concern  $U \in \mathcal{G}_h^2$ ,  $h \in (0, \frac{3}{2L})$ , satisfying

$$\begin{aligned} \frac{3}{2}U^j - 2U^{j-1} + \frac{1}{2}U^{j-2} &= hf(U^j) + \frac{3}{2}g(U^{j-1})\Delta_h W^j \\ &\quad - \frac{1}{2}g(U^{j-2})\Delta_h W^{j-1}, \quad j \in \{2, \dots, N_h\}, \end{aligned} \quad (5.1)$$

with initial values  $U^\ell \in L^2(\Omega, \mathcal{F}_{t_\ell}, \mathbf{P}; \mathbf{R}^m)$  such that  $f(U^\ell) \in L^2(\Omega, \mathcal{F}_{t_\ell}, \mathbf{P}; \mathbf{R}^m)$  and  $g(U^\ell) \in L^2(\Omega, \mathcal{F}_{t_\ell}, \mathbf{P}; \mathbf{R}^{m \times d})$  for  $\ell \in \{0, 1\}$ . Here  $L$  is the parameter of Assumption 2.1 and from Theorem 3.1 there exists for every  $h \in (0, \frac{3}{2L})$  a unique  $U \in \mathcal{G}_h^2$  satisfying (5.1). The initial values  $(U^0, U^1)$  are not necessarily related to the initial value  $X_0$  of (1.1).

Next, we state an analogue of Lemma 4.1, used for the proof of the a priori estimate in Theorem 5.1 and the stability result in Theorem 5.2.

**Lemma 5.1** For all  $h \in (0, \frac{3}{2L})$  and  $U, V \in \mathcal{G}_h^2$  with  $U$  satisfying (5.1) it holds for all  $j \in \{2, \dots, N_h\}$   $\mathbf{P}$ -almost surely that

$$\begin{aligned} & |E^j|^2 - |E^{j-1}|^2 + |2E^j - E^{j-1}|^2 - |2E^{j-1} - E^{j-2}|^2 + |E^j - 2E^{j-1} + E^{j-2}|^2 \\ &= 4h(f(U^j), E^j) + 2(g(U^{j-1})\Delta_h W^j - g(U^{j-2})\Delta_h W^{j-1}, E^j - 2E^{j-1} + E^{j-2}) \\ &\quad + 2(g(U^{j-1})\Delta_h W^j, 2E^j - E^{j-1}) - 2(g(U^{j-2})\Delta_h W^{j-1}, 2E^{j-1} - E^{j-2}) \\ &\quad - 4\left(\frac{3}{2}V^j - 2V^{j-1} + \frac{1}{2}V^{j-2}, E^j\right) + Z^j, \end{aligned}$$

where  $E := U - V$  and  $(Z^j)_{j \in \{2, \dots, N_h\}}$ , are the centered random variables given by

$$Z^j := (g(U^{j-1})\Delta_h W^j, 6E^{j-1} - 2E^{j-2}).$$

*Proof* From the identity (1.6) and since  $U$  satisfy (5.1) by assumption it holds for  $j \in \{2, \dots, N_h\}$  that

$$\begin{aligned} & |E^j|^2 - |E^{j-1}|^2 + |2E^j - E^{j-1}|^2 - |2E^{j-1} - E^{j-2}|^2 + |E^j - 2E^{j-1} + E^{j-2}|^2 \\ &= 4\left(\frac{3}{2}E^j - 2E^{j-1} + \frac{1}{2}E^{j-2}, E^j\right) \\ &= 4\left(\frac{3}{2}U^j - 2U^{j-1} + \frac{1}{2}U^{j-2}, E^j\right) - 4\left(\frac{3}{2}V^j - 2V^{j-1} + \frac{1}{2}V^{j-2}, E^j\right) \\ &= 4h(f(U^j), E^j) + 6(g(U^{j-1})\Delta_h W^j, E^j) - 2(g(U^{j-2})\Delta_h W^{j-1}, E^j) \\ &\quad - 4\left(\frac{3}{2}V^j - 2V^{j-1} + \frac{1}{2}V^{j-2}, E^j\right). \end{aligned}$$

Adding, subtracting and rearranging terms completes the proof of the asserted identity. Further note that  $Z^j$  is centered due to the independence of the centered Wiener increment  $\Delta_h W^j$  from  $g(U^{j-1})$ ,  $E^{j-1}$ , and  $E^{j-2}$ .  $\square$

**Theorem 5.1** Let Assumption 2.1 hold with  $L \in (0, \infty)$ ,  $\eta \in [\frac{1}{2}, \infty)$ ,  $q \in [1, \infty)$ . For  $h \in (0, \frac{1}{4L})$  denote by  $U \in \mathcal{G}_h^2$  the unique adapted grid function satisfying (5.1). Then, for all  $n \in \{2, \dots, N_h\}$  it holds that

$$\begin{aligned} & \|U^n\|^2 + h\|g(U^n)\|^2 \\ & \leq C_h \exp\left(\frac{4Lt_n}{1-4Lh}\right) \left(1 + \|U^1\|^2 + \|2U^1 - U^0\|^2 + \sum_{l=0}^1 \|g(U^l)\|^2\right), \end{aligned}$$

where  $C_h = 4 \max\{1, LT\}(1-4Lh)^{-1}$ .

*Proof* Applying Lemma 5.1 with  $V = 0$  and taking expectations yields

$$\begin{aligned} & \|U^j\|^2 - \|U^{j-1}\|^2 + \|2U^j - U^{j-1}\|^2 - \|2U^{j-1} - U^{j-2}\|^2 + \|U^j - 2U^{j-1} + U^{j-2}\|^2 \\ &= 4h\langle f(U^j), U^j \rangle + 2\langle g(U^{j-1})\Delta_h W^j - g(U^{j-2})\Delta_h W^{j-1}, U^j - 2U^{j-1} + U^{j-2} \rangle \\ &\quad + 2\langle g(U^{j-1})\Delta_h W^j, 2U^j - U^{j-1} \rangle - 2\langle g(U^{j-2})\Delta_h W^{j-1}, 2U^{j-1} - U^{j-2} \rangle. \end{aligned}$$

From the Young inequality (2.8), the orthogonality

$$\|g(U^{j-1})\Delta_h W^j - g(U^{j-2})\Delta_h W^{j-1}\|^2 = h\|g(U^{j-1})\|^2 + h\|g(U^{j-2})\|^2,$$

and the coercivity condition (2.3) we have that

$$\begin{aligned} & \|U^j\|^2 - \|U^{j-1}\|^2 + \|2U^j - U^{j-1}\|^2 - \|2U^{j-1} - U^{j-2}\|^2 \\ & \leq 4h\left(L(1 + \|U^j\|^2) - \frac{4q-3}{2}\|g(U^j)\|^2\right) + h\|g(U^{j-1})\|^2 + h\|g(U^{j-2})\|^2 \\ & \quad + 2\langle g(U^{j-1})\Delta_h W^j, 2U^j - U^{j-1} \rangle - 2\langle g(U^{j-2})\Delta_h W^{j-1}, 2U^{j-1} - U^{j-2} \rangle. \end{aligned}$$

Summing over  $j$  from 2 to  $n$ , identifying three telescoping sums, using the Young inequality (2.8) gives that

$$\begin{aligned} & \|U^n\|^2 + \|2U^n - U^{n-1}\|^2 \\ & \leq 4LT + \|U^1\|^2 + \|2U^1 - U^0\|^2 + 4Lh \sum_{j=2}^n \|U^j\|^2 - (8q-6)h \sum_{j=2}^n \|g(U^j)\|^2 \\ & \quad + h \sum_{j=1}^{n-1} \|g(U^j)\|^2 + h \sum_{j=0}^{n-2} \|g(U^j)\|^2 + h\|g(U^{n-1})\|^2 + \|2U^n - U^{n-1}\|^2 \\ & \quad + h\|g(U^0)\|^2 + \|2U^1 - U^0\|^2. \end{aligned}$$

This yields

$$\begin{aligned} & (1 - 4Lh)\|U^n\|^2 + (8q-6)h\|g(U^n)\|^2 \\ & \leq 4LT + \|U^1\|^2 + 2\|2U^1 - U^0\|^2 + 2h \sum_{l=0}^1 \|g(U^l)\|^2 \\ & \quad + (8-8q)h \sum_{j=2}^{n-1} \|g(U^j)\|^2 + 4Lh \sum_{j=2}^{n-1} \|U^j\|^2. \end{aligned}$$

Since  $q \in [1, \infty)$  it holds  $8-8q \leq 0$  and  $8q-6 \geq 2$ . By elementary bounds we get

$$\begin{aligned} & \|U^n\|^2 + h\|g(U^n)\|^2 \leq \frac{4L}{1-4Lh} h \sum_{j=2}^{n-1} \|U^j\|^2 \\ & \quad + \frac{1}{1-4Lh} \left(4LT + \|U^1\|^2 + 2\|2U^1 - U^0\|^2 + 2h \sum_{l=0}^1 \|g(U^l)\|^2\right). \end{aligned}$$

We conclude by a use of the discrete Gronwall Lemma (2.9).  $\square$

## 5.2 Stability of the BDF2-Maruyama scheme

Similar to the stability of the BEM scheme, for  $h \in (0, 1)$ ,  $V \in \mathcal{G}_h^2$  we define the local truncation error of  $V$  by

$$\begin{aligned} \rho_h^{\text{BDF2}}(V) &:= \max_{j \in \{1, \dots, N_h\}} \frac{1}{h} \|\rho_{1,h}^j(V)\|^2 + \sum_{j=2}^{N_h} \|\rho_{2,h}^j(V) + \rho_{3,h}^j(V)\|^2 \\ &\quad + \frac{1}{h} \sum_{j=2}^{N_h} \|\rho_h^{j-1} \rho_{2,h}^j(V)\|^2 + \frac{1}{h} \sum_{j=2}^{N_h} \|\rho_h^{j-2} \rho_{3,h}^j(V)\|^2, \end{aligned} \quad (5.2)$$

where

$$\begin{aligned} \rho_{1,h}^j(V) &:= hf(V^j) + g(V^{j-1})\Delta_h W^j - V^j + V^{j-1}, \\ \rho_{2,h}^j(V) &:= \frac{1}{2}(hf(V^{j-1}) + g(V^{j-1})\Delta_h W^j - V^j + V^{j-1}), \\ \rho_{3,h}^j(V) &:= -\frac{1}{2}(hf(V^{j-1}) + g(V^{j-2})\Delta_h W^{j-1} - V^{j-1} + V^{j-2}), \end{aligned} \quad (5.3)$$

for  $j \in \{2, \dots, N_h\}$ . Similar to (4.3) we define the maximal step size

$$h_B = \frac{1}{2(4L+1)}.$$

Note that the proof of Theorem 5.1 indicates that the assertion of the following theorem actually holds true for all  $h \in (0, \frac{1}{4L})$  but the constants on the right hand side then depend on  $\frac{1}{1-4hL}$ .

**Theorem 5.2** *Let Assumption 2.1 hold with  $L \in (0, \infty)$ ,  $\eta \in (\frac{1}{2}, \infty)$ . For all  $h \in (0, h_B]$ ,  $U \in \mathcal{G}_h^2$  satisfying (5.1),  $V \in \mathcal{G}_h^2$ , and all  $n \in \{2, \dots, N_h\}$  it holds that*

$$\begin{aligned} &\|U^n - V^n\|^2 + h \|g(U^n) - g(V^n)\|^2 \\ &\leq C \exp\left(4 \max\left\{(1+2L), \frac{\eta}{2\eta-1}\right\} t_n\right) \\ &\quad \times \left(\sum_{\ell=0}^1 (\|U^\ell - V^\ell\|^2 + h \|g(U^\ell) - g(V^\ell)\|^2) + \rho_h^{\text{BDF2}}(V)\right), \end{aligned}$$

where  $C = \max\{30, 4\eta + 2, \frac{16\eta}{2\eta-1}\}$ .

*Proof* Fix arbitrary  $h \in (0, h_B]$  and  $V \in \mathcal{G}_h^2$ . We reuse the notation from the proof of Theorem 4.2. In particular we set  $E := U - V$  and we often suppress  $h$  from the notation. The local residual of  $V$  is given by

$$\rho^j := hf(V^j) + \frac{3}{2}g(V^{j-1})\Delta W^j - \frac{1}{2}g(V^{j-2})\Delta W^{j-1} - \frac{3}{2}V^j + 2V^{j-1} - \frac{1}{2}V^{j-2},$$

for  $j \in \{2, \dots, N_h\}$ . From Lemma 5.1 we get after taking expectations that

$$\begin{aligned} & \|E^j\|^2 - \|E^{j-1}\|^2 + \|2E^j - E^{j-1}\|^2 - \|2E^{j-1} - E^{j-2}\|^2 + \|E^j - 2E^{j-1} + E^{j-2}\|^2 \\ &= 4\langle \Delta f^j, E^j \rangle + 2\langle \Delta g^{j-1} \Delta W^j - \Delta g^{j-2} \Delta W^{j-1}, E^j - 2E^{j-1} + E^{j-2} \rangle + 4\langle \rho^j, E^j \rangle \\ & \quad + 2\langle \Delta g^{j-1} \Delta W^j, 2E^j - E^{j-1} \rangle - 2\langle \Delta g^{j-2} \Delta W^{j-1}, 2E^{j-1} - E^{j-2} \rangle. \end{aligned}$$

We observe that  $P_h^{j-1}(2E^{j-1} - E^{j-2}) = 2E^{j-1} - E^{j-2}$  and  $P_h^{j-2}E^{j-2} = E^{j-2}$ . Further, we decompose the local residual of  $V$  by

$$\rho^j = \rho_1^j + \rho_2^j + \rho_3^j, \quad (5.4)$$

where  $\rho_i^j := \rho_i^j(V)$ ,  $i \in \{1, 2, 3\}$ , are defined in (5.3). Then, by taking the adjoints of the projectors and by applying the weighted Young inequality (2.8) with  $\nu = \mu > 0$  and with  $\nu = h > 0$ , respectively, and by noting that  $-2\rho_3^j = \rho_1^{j-1}$ , we obtain

$$\begin{aligned} \langle \rho^j, E^j \rangle &= \langle \rho_1^j, E^j \rangle + \langle \rho_2^j + \rho_3^j, E^j - 2E^{j-1} + E^{j-2} \rangle + \langle \rho_2^j + \rho_3^j, 2E^{j-1} - E^{j-2} \rangle \\ &\leq \langle \rho_1^j, E^j \rangle + \frac{\mu}{2} \|\rho_2^j + \rho_3^j\|^2 + \frac{1}{2\mu} \|E^j - 2E^{j-1} + E^{j-2}\|^2 \\ & \quad + \langle \rho_2^j, P_h^{j-1}(2E^{j-1} - E^{j-2}) \rangle + \langle \rho_3^j, 2E^{j-1} \rangle - \langle \rho_3^j, P_h^{j-2}E^{j-2} \rangle \\ &\leq \langle \rho_1^j, E^j \rangle - \langle \rho_1^{j-1}, E^{j-1} \rangle + \frac{\mu}{2} \|\rho_2^j + \rho_3^j\|^2 + \frac{1}{2\mu} \|E^j - 2E^{j-1} + E^j\|^2 \\ & \quad + \frac{1}{2h} \|P_h^{j-1}\rho_2^j\|^2 + \frac{h}{2} \|2E^{j-1} - E^{j-2}\|^2 + \frac{1}{2h} \|P_h^{j-2}\rho_3^j\|^2 + \frac{h}{2} \|E^{j-2}\|^2. \end{aligned}$$

Together with the global monotonicity condition (2.1) and the weighted Young inequality (2.8) with  $\nu = 2\eta$  this gives that

$$\begin{aligned} & \|E^j\|^2 - \|E^{j-1}\|^2 + \|2E^j - E^{j-1}\|^2 - \|2E^{j-1} - E^{j-2}\|^2 \\ &\leq 4hL\|E^j\|^2 - 4h\eta\|\Delta g^j\|^2 + 2\eta h\|\Delta g^{j-1}\|^2 + 2\eta h\|\Delta g^{j-2}\|^2 \\ & \quad + \left(\frac{2}{\mu} + \frac{1}{2\eta} - 1\right) \|E^j - 2E^{j-1} + E^{j-2}\|^2 + 2h\|2E^{j-1} - E^{j-2}\|^2 + 2h\|E^{j-2}\|^2 \\ & \quad + 2\langle \Delta g^{j-1} \Delta W^j, 2E^j - E^{j-1} \rangle - 2\langle \Delta g^{j-2} \Delta W^{j-1}, 2E^{j-1} - E^{j-2} \rangle \\ & \quad + 4\langle \rho_1^j, E^j \rangle - 4\langle \rho_1^{j-1}, E^{j-1} \rangle + 2\mu \|\rho_2^j + \rho_3^j\|^2 + \frac{2}{h} \|P_h^{j-1}\rho_2^j\|^2 + \frac{2}{h} \|P_h^{j-2}\rho_3^j\|^2. \end{aligned}$$

Setting  $\mu = \frac{4\eta}{2\eta-1} > 0$  gives that  $\frac{2}{\mu} + \frac{1}{2\eta} - 1 = 0$ . Then, summing over  $j$  from 2 to  $n$  and identifying four telescoping sums yields

$$\begin{aligned} & \|E^n\|^2 + \|2E^n - E^{n-1}\|^2 \\ & \leq \|E^1\|^2 + \|2E^1 - E^0\|^2 + 4hL \sum_{j=2}^n \|E^j\|^2 - 4\eta h \sum_{j=2}^n \|\Delta g^j\|^2 + 2\eta h \sum_{j=1}^{n-1} \|\Delta g^j\|^2 \\ & \quad + 2\eta h \sum_{j=0}^{n-2} \|\Delta g^j\|^2 + 2h \sum_{j=1}^{n-1} \|2E^j - E^{j-1}\|^2 + 2h \sum_{j=0}^{n-2} \|E^j\|^2 \\ & \quad + 2\langle \Delta g^{n-1} \Delta W^n, 2E^n - E^{n-1} \rangle - 2\langle \Delta g^0 \Delta W^1, 2E^1 - E^0 \rangle + 4\langle \rho_1^n, E^n \rangle \\ & \quad - 4\langle \rho_1^1, E^1 \rangle + \frac{8\eta}{2\eta-1} \sum_{j=2}^n \|\rho_2^j + \rho_3^j\|^2 + \frac{2}{h} \sum_{j=2}^n \|P_h^{j-1} \rho_2^j\|^2 + \frac{2}{h} \sum_{j=2}^n \|P_h^{j-2} \rho_3^j\|^2. \end{aligned}$$

Next, we get from the weighted Young inequality (2.8) with  $v = \frac{2}{h}$  that  $4\langle \rho_1^n, E^n \rangle \leq \frac{4}{h} \|\rho_1^n\|^2 + h \|E^n\|^2$ . A further application of the weighted Young inequality (2.8) with  $v = 2\eta$  yields

$$\begin{aligned} & (1 - (4L+1)h) \|E^n\|^2 + \left(1 - \frac{1}{2\eta}\right) \|2E^n - E^{n-1}\|^2 \\ & \leq (1+h) \|E^1\|^2 + (1+h) \|2E^1 - E^0\|^2 + 4hL \sum_{j=2}^n \|E^j\|^2 - 4\eta h \sum_{j=2}^n \|\Delta g^j\|^2 \\ & \quad + 2\eta h \sum_{j=1}^{n-1} \|\Delta g^j\|^2 + 2\eta h \sum_{j=0}^{n-2} \|\Delta g^j\|^2 + 2h \sum_{j=1}^{n-1} \|2E^j - E^{j-1}\|^2 + 2h \sum_{j=0}^{n-2} \|E^j\|^2 \\ & \quad + 2\eta h \|\Delta g^{n-1}\|^2 + h \|\Delta g^0\|^2 + \frac{4}{h} \|\rho_1^n\|^2 + \frac{4}{h} \|\rho_1^1\|^2 + \frac{8\eta}{2\eta-1} \sum_{j=2}^n \|\rho_2^j + \rho_3^j\|^2 \\ & \quad + \frac{2}{h} \sum_{j=2}^n \|P_h^{j-1} \rho_2^j\|^2 + \frac{2}{h} \sum_{j=2}^n \|P_h^{j-2} \rho_3^j\|^2. \end{aligned}$$

At this point we notice that

$$\begin{aligned} & 2\eta h \sum_{j=1}^{n-1} \|\Delta g^j\|^2 + 2\eta h \sum_{j=0}^{n-2} \|\Delta g^j\|^2 + 2\eta h \|\Delta g^{n-1}\|^2 + h \|\Delta g^0\|^2 - 4\eta h \sum_{j=2}^n \|\Delta g^j\|^2 \\ & \leq -4\eta h \|\Delta g^n\|^2 + (2\eta+1)h \|\Delta g^0\|^2 + 4\eta h \|\Delta g^1\|^2. \end{aligned}$$

In addition, since  $1 - h(4L+1) > 1 - h_B(4L+1) = \frac{1}{2}$  and  $h \leq h_B < \frac{1}{2}$  and  $\eta > \frac{1}{2}$  as well as  $\|2E^1 + E^0\|^2 \leq 5(\|E^1\|^2 + \|E^0\|^2)$  we obtain after some elementary transformations the inequality

$$\begin{aligned} & \|E^n\|^2 + \frac{2\eta-1}{\eta} \|2E^n - E^{n-1}\|^2 + h \|\Delta g^n\|^2 \leq \max \left\{ 30, 4\eta + 2, \frac{16\eta}{2\eta-1} \right\} \\ & \quad \times \left( \|E^0\|^2 + \|E^1\|^2 + h \|\Delta g^0\|^2 + h \|\Delta g^1\|^2 + \rho_h^{\text{BDF}^2}(V) \right) \\ & \quad + 4 \max \left\{ (1+2L), \frac{\eta}{2\eta-1} \right\} h \sum_{j=2}^{n-1} \left( \|E^j\|^2 + \frac{2\eta-1}{\eta} \|2E^j - E^{j-1}\|^2 \right). \end{aligned}$$

The proof is completed by an application of (2.9).  $\square$

### 5.3 Consistency of the BDF2 scheme

In this subsection we bound the local truncation error of the exact solution.

**Theorem 5.3** *Let Assumption 2.1 hold and let  $X$  be the solution to (1.1). Then there exists  $C > 0$  such that*

$$\rho_h^{\text{BDF2}}(X|\tau_h) \leq Ch, \quad h \in (0, 1).$$

*Proof* In this proof we write  $\rho_i^j := \rho_{h,i}^j(X|\tau_h)$ ,  $i \in \{1, 2, 3\}$ ,  $j \in \{2, \dots, N_h\}$ ,  $h \in (0, 1)$ . From the definition of  $\rho_h$  we see that it suffices to show that

$$\max_{j \in \{2, \dots, N_h\}} \left( \|\rho_1^j\|^2 + \|\rho_2^j + \rho_3^j\|^2 + \frac{1}{h} \|P_h^{j-1} \rho_2^j\|^2 + \frac{1}{h} \|P_h^{j-2} \rho_3^j\|^2 \right) \leq Ch^2. \quad (5.5)$$

It holds for  $j \in \{2, \dots, N_h\}$  that

$$\begin{aligned} \rho_1^j &= \int_{t_{j-1}}^{t_j} (f(X(t_j)) - f(X(s))) \, ds + \int_{t_{j-1}}^{t_j} (g(X(t_{j-1})) - g(X(s))) \, dW(s), \\ \rho_2^j + \rho_3^j &= \frac{1}{2} \left( \int_{t_{j-1}}^{t_j} (g(X(t_{j-1})) - g(X(s))) \, dW(s) - \int_{t_{j-1}}^{t_j} f(X(s)) \, ds \right. \\ &\quad \left. - \int_{t_{j-2}}^{t_{j-1}} (g(X(t_{j-2})) - g(X(s))) \, dW(s) + \int_{t_{j-2}}^{t_{j-1}} f(X(s)) \, ds \right), \\ P_h^{j-1} \rho_2^j &= \frac{1}{2} \mathbf{E} \left[ \int_{t_{j-1}}^{t_j} (f(X(t_{j-1})) - f(X(s))) \, ds \mid \mathcal{F}_{t_{j-1}} \right], \\ P_h^{j-2} \rho_3^j &= -\frac{1}{2} \mathbf{E} \left[ \int_{t_{j-2}}^{t_{j-1}} (f(X(t_{j-2})) - f(X(s))) \, ds \mid \mathcal{F}_{t_{j-2}} \right]. \end{aligned}$$

As in the proof of Theorem 4.3, we note that the estimates (4.5) and (4.6) are applicable to (5.5) due to the moment bound (2.4). We further make use of the fact that  $\|\mathbf{E}[V | \mathcal{F}_{t_{j-1}}]\| \leq \|V\|$  for every  $V \in L^2(\Omega; \mathbf{R}^m)$  and the bound

$$\left\| \int_{\tau_1}^{\tau_2} f(X(s)) \, ds \right\| \leq C \left( 1 + \sup_{t \in [0, T]} \|X(t)\|_{L^{2q}(\Omega; \mathbf{R}^m)}^q \right) |\tau_2 - \tau_1|, \quad t_1, t_2 \in [0, T],$$

which is obtained from (2.5). By these estimates and an application of the triangle inequality we directly deduce (5.5).  $\square$

### 5.4 Mean-square convergence of the BDF2 scheme

Here we consider the numerical approximations  $(X_h^j)_{j=0}^{N_h}$ ,  $h \in (0, h_B]$ ,  $h_B = \frac{1}{\max\{8L, 2\}}$ , which are uniquely determined by the backward difference formula (1.3) and a family of initial values  $(X_h^0, X_h^1)_{h \in (0, h_B]}$ . This family is assumed to satisfy the following assumption.

**Assumption 5.1** The family of initial values  $(X_h^0, X_h^1)_{h \in (0, h_B]}$  satisfies

$$X_h^\ell, f(X_h^\ell) \in L^2(\Omega, \mathcal{F}_{t_\ell}, \mathbf{P}; \mathbf{R}^m), \quad g(X_h^\ell) \in L^2(\Omega, \mathcal{F}_{t_\ell}, \mathbf{P}; \mathbf{R}^{m \times d}), \quad (5.6)$$

for all  $h \in (0, h_B]$ ,  $\ell \in \{0, 1\}$ , and is consistent of order  $\frac{1}{2}$  in the sense that

$$\sum_{\ell=0}^1 \|X(h\ell) - X_h^\ell\|^2 + h \sum_{\ell=0}^1 \|g(X(h\ell)) - g(X_h^\ell)\|^2 = \mathcal{O}(h), \quad (5.7)$$

as  $h \downarrow 0$ , where  $X$  is the solution to (1.1).

We are now ready to state the main result of this section.

**Theorem 5.4** *Let Assumptions 2.1 and 5.1 hold, let  $X$  be the solution to (1.1) and  $(X_h^j)_{j=0}^{N_h}$ ,  $h \in (0, h_B]$ , the solutions to (1.3) with initial values  $(X_h^0, X_h^1)_{h \in (0, h_B]}$ . Under these conditions the BDF2-Maruyama method is mean-square convergent of order  $\frac{1}{2}$ , more precisely, there exists  $C > 0$  such that*

$$\max_{n \in \{0, \dots, N_h\}} \|X_h^n - X(nh)\| \leq C\sqrt{h}, \quad h \in (0, h_B].$$

*Proof* For  $h \in (0, h_B]$ , we apply Theorem 5.2 with  $U = (X_h^j)_{j=0}^{N_h} \in \mathcal{G}_h^2$  and  $V = X|_{\tau_h} = (X(t_j))_{j=0}^{N_h} \in \mathcal{G}_h^2$  and get that there is a constant  $C > 0$ , independent of  $h$ , such that

$$\begin{aligned} & \|X_h^n - X(nh)\|^2 \\ & \leq C \left( \sum_{\ell=0}^1 \|X_h^\ell - X(h\ell)\|^2 + h \sum_{\ell=0}^1 \|g(X_h^\ell) - g(X(h\ell))\|^2 + \rho_h^{\text{BDF2}}(X|_{\tau_h}) \right). \end{aligned}$$

The sums are of order  $\mathcal{O}(h)$  by (5.7). In addition, the consistency term  $\rho_h^{\text{BDF2}}(X|_{\tau_h})$  is also of order  $\mathcal{O}(h)$  by Theorem 5.3.  $\square$

### 5.5 Admissible initial values for the BDF2-Maruyama scheme

Assumption 5.1 provides an abstract criterion for an admissible choice of the initial values for the BDF2-Maruyama method such that the mean-square convergence of order  $\frac{1}{2}$  is ensured. Here we consider a concrete scheme for the computation of the second initial value, namely the computation of  $X_h^1$  by one step of the backward Euler-Maruyama method.

**Theorem 5.5** *Let Assumption 2.1 be fulfilled. Consider a family  $(X_h^0)_{h \in (0, h_B]}$  of approximate initial values satisfying Assumption 4.1. If  $(X_h^1)_{h \in (0, h_B]}$  is determined by one step of the backward Euler-Maruyama method, i.e. if for all  $h \in (0, h_B]$  the random variable  $X_h^1$  solves the equation*

$$X_h^1 = X_h^0 + hf(X_h^1) + g(X_h^0)\Delta_h W^1,$$

*then  $(X_h^0, X_h^1)_{h \in (0, h_B]}$  satisfy the conditions of Assumption 5.1.*

*Proof* The fact that the solution of (1.2) belongs to  $\mathcal{G}_h^2$  proves (5.6) of Assumption 5.1. By Theorem 4.2 it holds that

$$\begin{aligned} & \sum_{\ell=0}^1 \|X(t_\ell) - X_h^\ell\|^2 + h \sum_{\ell=0}^1 \|g(X(t_\ell)) - g(X_h^\ell)\|^2 \\ & \leq (1 + Ce^{2(1+2L)h}) \left( \|X(0) - X_h^0\|^2 + h \|g(X(0)) - g(X_h^0)\|^2 + \rho_h^{\text{BEM}}(X|_{\tau_h}) \right). \end{aligned}$$

From Theorem 4.3 and Assumption 4.1 the right hand side is of order  $\mathcal{O}(h)$  as  $h \downarrow 0$ , and this proves (5.7).  $\square$

*Remark 5.1* Consider the same assumption as in Theorem 5.5. From the Hölder continuity of the solution  $X$  of (1.1) and Assumption 4.1 it holds that

$$\|X(h) - X_h^0\| \leq \|X(h) - X(0)\| + \|X(0) - X_h^0\| \leq C\sqrt{h}.$$

Therefore, also the choice  $X_h^1 := X_h^0$  satisfies the conditions of Assumption 5.1 and, therefore, is feasible in terms of the asymptotic rate of convergence. However, numerical simulations similar to those in Section 6 indicate that, although the experimental convergence rates behave as expected, this simple choice of the second initial value leads to a significantly larger error compared to  $X_h^1$  being generated by one step of the backward Euler-Maruyama method.

## 6 Numerical experiments

In this section we perform some numerical experiments which illustrate the theoretical results from the previous sections. In Subsection 6.1 we consider the  $\frac{3}{2}$ -volatility model from finance, which is a one dimensional equation. In Subsection 6.2 we do computations for a two dimensional dynamics which mimics the form and properties of the discretization of a stochastic partial differential equation, like the Allen-Cahn equation.

### 6.1 An example in one dimension: the $\frac{3}{2}$ -volatility model

Hereby we consider the stochastic differential equation

$$\begin{aligned} dX(t) &= [X(t) - \lambda X(t)|X(t)|] dt + \sigma |X(t)|^{\frac{3}{2}} dW(t), \quad t \in [0, T], \\ X(0) &= X_0, \end{aligned} \quad (6.1)$$

with  $m = d = 1$ ,  $\lambda > 0$ ,  $\sigma \in \mathbf{R}$ , and  $X_0 \in \mathbf{R}$ . For positive initial conditions this equation is also known as the  $\frac{3}{2}$ -volatility model [5, 6]. From the quadratic growth of the drift it holds that  $q = 2$  in Assumption 2.1 and, as the reader can check, the coercivity condition (2.3) is valid for  $L = 1$  provided that  $\lambda \geq \frac{4q-3}{2}\sigma^2 = \frac{5}{2}\sigma^2$ . From the calculation in [19, Appendix] it holds for all  $x_1, x_2 \in \mathbf{R}$  that

$$\begin{aligned} & (f(x_1) - f(x_2), x_1 - x_2) + \eta |g(x_1) - g(x_2)|^2 \\ & \leq |x_1 - x_2|^2 + (2\sigma^2\eta - \lambda)(|x_1| + |x_2|)(|x_1| - |x_2|)^2. \end{aligned}$$

The global monotonicity condition (2.1) is therefore satisfied with  $L = 1$  and  $\eta \leq \frac{\lambda}{2\sigma^2}$ . As we require  $\eta > \frac{1}{2}$  this imposes the condition  $\lambda > \sigma^2$  and altogether we have that Assumption 2.1 is valid for  $L = 1$ ,  $q = 2$ ,  $\eta \in (\frac{1}{2}, \frac{\lambda}{2\sigma^2})$  provided that  $\lambda \geq \frac{5}{2}\sigma^2$ .

In our experiments we approximate the strong error of convergence for the explicit Euler-Maruyama method (EulM) (see [13]), the backward Euler-Maruyama method (BEM), and the BDF2-Maruyama method (BDF2), respectively. More precisely, we approximate the root mean square error by a Monte Carlo simulation based on  $M = 10^6$  samples, that is

$$\text{error}(h) := \max_{0 \leq n \leq N_h} \left( \frac{1}{M} \sum_{m=1}^M |X^{(m)}(nh) - X_h^{n,(m)}|^2 \right)^{\frac{1}{2}} \approx \max_{0 \leq n \leq N_h} \|X(nh) - X_h^n\|,$$

where for every  $m \in \{1, \dots, M\}$  the processes  $X^{(m)}$  and  $(X_h^{n,(m)})_{n=0}^{N_h}$  denote independently generated copies of  $X$  and  $X_h$ , respectively. Here we set  $h := \frac{T}{N_h}$  and for the number of steps  $N_h$  we use the values  $\{25 \cdot 2^k : k = 0, \dots, 7\}$ , i.e.,  $N_h$  ranges from 25 to 3200. Since there is no explicit expression of the exact solution to (6.1) available, we replace  $X^{(m)}$  in the error computation by a numerical reference solution generated by the BDF2-Maruyama method with  $N_{\text{ref}} = 25 \cdot 2^{12}$  steps.

As already discussed in Section 3, in every time step of the implicit schemes we have to solve a nonlinear equation of the form

$$X_h^j - h\beta f(X_h^j) = R_h^j, \quad (6.2)$$

for  $X_h^j$ . Here, we have  $f(x) = x - \lambda x|x|$  and  $g(x) = \sigma|x|^{\frac{3}{2}}$  for  $x \in \mathbf{R}$  and

$$\beta = 1, \quad R_h^j = X_h^{j-1} + g(X_h^{j-1})\Delta_h W^j, \quad (6.3)$$

for the backward Euler-Maruyama method, and

$$\beta = \frac{2}{3}, \quad R_h^j = \frac{4}{3}X_h^{j-1} - \frac{1}{3}X_h^{j-2} + g(X_h^{j-1})\Delta_h W^j - \frac{1}{3}g(X_h^{j-2})\Delta_h W^{j-1}, \quad (6.4)$$

for the BDF2-Maruyama method. For the  $\frac{3}{2}$ -volatility model it turns out that (6.2) is a simple quadratic equation, which can be solved explicitly. Depending on the sign of the right hand side  $X_h^j$  is given by

$$X_h^j = \begin{cases} -\frac{1-\beta h}{2\beta h\lambda} + \left( \left( \frac{1-\beta h}{2\beta h\lambda} \right)^2 + \frac{R_h^j}{\beta h\lambda} \right)^{\frac{1}{2}}, & \text{if } R_h^j \geq 0, \\ \frac{1-\beta h}{2\beta h\lambda} - \left( \left( \frac{1-\beta h}{2\beta h\lambda} \right)^2 - \frac{R_h^j}{\beta h\lambda} \right)^{\frac{1}{2}}, & \text{if } R_h^j < 0. \end{cases}$$

As the first initial value we set  $X_h^0 \equiv X_0$  for both schemes. In addition, we generate the second initial value for the BDF2-Maruyama method by one step of the BEM method as proposed in Section 5.5. Note that the computation of one step of the BDF2-Maruyama method is, up to some additional operations needed for the evaluation of  $R_h^j$ , as costly as one step of the BEM method.

**Table 6.1** Non-stiff case without noise:  $\lambda = 4$ ,  $\sigma = 0$ .

$N_h$	EulM		BEM		BDF2	
	error	EOC	error	EOC	error	EOC
25	0.024635		0.020186		0.010594	
50	0.011619	1.08	0.010528	0.94	0.003739	1.50
100	0.005659	1.04	0.005388	0.97	0.001134	1.72
200	0.002793	1.02	0.002726	0.98	0.000325	1.80
400	0.001388	1.01	0.001371	0.99	0.000088	1.89
800	0.000692	1.00	0.000688	1.00	0.000023	1.93
1600	0.000345	1.00	0.000344	1.00	0.000006	1.96
3200	0.000173	1.00	0.000172	1.00	0.000002	1.98

**Table 6.2** Non-stiff case with smaller noise intensity:  $\lambda = 4$ ,  $\sigma = \frac{1}{3}$ .

$N_h$	EulM		BEM		BDF2	
	error	EOC	error	EOC	error	EOC
25	0.026853		0.020812		0.011949	
50	0.012788	1.07	0.011020	0.92	0.004961	1.27
100	0.006398	1.00	0.005816	0.92	0.002662	0.90
200	0.003334	0.94	0.003115	0.90	0.001695	0.65
400	0.001818	0.87	0.001733	0.85	0.001140	0.57
800	0.001051	0.79	0.001016	0.77	0.000785	0.54
1600	0.000647	0.70	0.000632	0.69	0.000546	0.52
3200	0.000417	0.63	0.000411	0.62	0.000380	0.52

**Table 6.3** Non-stiff case with higher noise intensity:  $\lambda = 4$ ,  $\sigma = 1$ .

$N_h$	EulM		BEM		BDF2	
	error	EOC	error	EOC	error	EOC
25	0.069083		0.048076		0.048450	
50	0.039639	0.80	0.032517	0.56	0.032775	0.56
100	0.024776	0.68	0.022244	0.55	0.022382	0.55
200	0.016454	0.59	0.015563	0.52	0.015617	0.52
400	0.011187	0.56	0.010873	0.52	0.010894	0.52
800	0.007770	0.53	0.007656	0.51	0.007665	0.51
1600	0.005412	0.52	0.005375	0.51	0.005377	0.51
3200	0.003790	0.51	0.003778	0.51	0.003778	0.51

In all simulations the initial condition of equation (6.1) is set to be  $X_0 = 1$ , while the length of the time interval equals  $T = 1$ . Regarding the choice of the noise intensity  $\sigma$  let us note that in the deterministic situation with  $\sigma = 0$  it is well-known that the BDF2 method converges with order 2 to the exact solution. In the stochastic case with  $\sigma > 0$ , however, the order of convergence reduces asymptotically to  $\frac{1}{2}$  due to the presence of the noise. Hence, the BDF2-Maruyama method offers apparently no advantage over the backward Euler-Maruyama method. But, as it has already been observed in [2], one still benefits from the higher deterministic order of convergence if the intensity of the noise is small compared to the step size of the numerical scheme. To illustrate this effect we use three different noise levels in our simulations: the de-

terministic case  $\sigma = 0$ , a small noise intensity with  $\sigma = \frac{1}{3}$ , and a higher intensity with  $\sigma = 1$ .

Moreover, the equation (6.1) behaves stiffer in the sense of numerical analysis if the value for  $\lambda$  is increased. Since implicit numerical schemes like the backward Euler method and the BDF2 method are known to behave more stable in this situation than explicit schemes, we will perform our simulations with two different values for  $\lambda$ : The non-stiff case with  $\lambda = 4$  and the stiff case with  $\lambda = 25$ . Note that the condition  $\lambda \geq \frac{5}{2}\sigma^2$  is satisfied for all combinations of  $\lambda$  and  $\sigma$ .

Further, to better illustrate the effect of the parameter  $\lambda$  on explicit schemes explains why we also included the explicit Euler-Maruyama method in our simulations. Although this scheme is actually known to be divergent for SDEs involving superlinearly growing drift- and diffusion coefficient functions, see [11], it nonetheless often yields reliable numerical results. But let us stress that the observed experimental convergence of the explicit Euler-Maruyama scheme is purely empirical and does not indicate its convergence in the sense of (1.4).

The first set of numerical results are displayed in Tables 6.1 to 6.3, which are concerned with the non-stiff case  $\lambda = 4$ . In Table 6.1 we see the errors computed in the deterministic case  $\sigma = 0$ . As expected the explicit Euler scheme and the backward Euler method perform equally well, while the experimental errors of the BDF2 method are much smaller. This is also indicated by the *experimental order of convergence* (EOC) which is defined for successive step sizes and errors by

$$\text{EOC} = \frac{\log(\text{error}(h_i)) - \log(\text{error}(h_{i-1}))}{\log(h_i) - \log(h_{i-1})}.$$

As expected the numerical results are in line with the theoretical orders.

In Table 6.2 the noise intensity is increased to  $\sigma = \frac{1}{3}$ . Here we see that for larger step sizes, that is  $N_h \in \{25, 50\}$ , the errors are only slightly larger than in the deterministic case. In fact, for the two Euler methods the discretization error of the drift part seems to dominate the total error for almost all step sizes as the errors mostly coincide with those in Table 6.1. On the other hand, the BDF2-Maruyama method performs significantly better for larger and medium sized step sizes. Only on the two finest refinement levels  $N_h \in \{1600, 3200\}$  the estimated errors of all three schemes are of the same magnitude. This picture changes drastically in Table 6.3, which shows the result of the same experiment but with  $\sigma = 1$ . Here the errors of all schemes agree for almost all step sizes and the BDF2-Maruyama method is no longer superior.

The second set of experiments shown in Tables 6.4 to 6.6 are concerned with the stiff case  $\lambda = 25$  while all other parameters remain unchanged. At first glance we see that the explicit Euler-Maruyama method performs much worse than the two implicit methods for  $N_h \in \{25, 50, 100, 200\}$  in the deterministic case  $\sigma = 0$ . This even stays true when noise is present. On the other hand, the BDF2 method clearly performs best in the deterministic case although the experimental order of convergence increases rather slowly to 2 compared to the non-stiff case in Table 6.1. Further note that the error of the BEM method and the BDF2 method agree for  $N_h = 25$ . This is explained by the fact that the second initial value of the multi-step method is generated by the BEM method and, apparently, this is where the error is largest for both schemes.

**Table 6.4** Stiff case without noise:  $\lambda = 25$ ,  $\sigma = 0$ .

$N_h$	EulM		BEM		BDF2	
	error	EOC	error	EOC	error	EOC
25	0.475184		0.114050		0.114050	
50	0.157860	1.59	0.067366	0.76	0.062722	0.86
100	0.054660	1.53	0.038126	0.82	0.027090	1.21
200	0.024244	1.17	0.020389	0.90	0.010049	1.43
400	0.011541	1.07	0.010594	0.94	0.003426	1.55
800	0.005640	1.03	0.005404	0.97	0.001017	1.75
1600	0.002789	1.02	0.002730	0.98	0.000289	1.81
3200	0.001387	1.01	0.001372	0.99	0.000078	1.90

**Table 6.5** Stiff case with smaller noise intensity:  $\lambda = 25$ ,  $\sigma = \frac{1}{3}$ .

$N_h$	EulM		BEM		BDF2	
	error	EOC	error	EOC	error	EOC
25	0.477006		0.114345		0.114345	
50	0.159402	1.58	0.067506	0.76	0.062802	0.86
100	0.055190	1.53	0.038191	0.82	0.027099	1.21
200	0.024422	1.18	0.020420	0.90	0.010129	1.42
400	0.011622	1.07	0.010614	0.94	0.003471	1.55
800	0.005679	1.03	0.005416	0.97	0.001074	1.69
1600	0.002811	1.01	0.002739	0.98	0.000351	1.61
3200	0.001401	1.00	0.001379	0.99	0.000182	0.95

**Table 6.6** Stiff case with higher noise intensity:  $\lambda = 25$ ,  $\sigma = 1$ .

$N_h$	EulM		BEM		BDF2	
	error	EOC	error	EOC	error	EOC
25	0.492313		0.117432		0.117432	
50	0.171504	1.52	0.069266	0.76	0.064308	0.87
100	0.060257	1.51	0.039290	0.82	0.028057	1.20
200	0.026558	1.18	0.021182	0.89	0.011774	1.25
400	0.012821	1.05	0.011208	0.92	0.005207	1.18
800	0.006477	0.98	0.005938	0.92	0.002991	0.80
1600	0.003414	0.92	0.003215	0.89	0.001922	0.64
3200	0.001897	0.85	0.001814	0.83	0.001295	0.57

Moreover, we observe that the errors in Table 6.5 with  $\sigma = \frac{1}{3}$  are of the same magnitude as those in Table 6.4. Due to the larger value of  $\lambda$  the presence of the noise only seems to have a visible impact on the error of the BDF2-Maruyama method with  $N_h = 3200$ . Hence, the BEM method performs significantly worse than the BDF2-Maruyama scheme for all larger values of  $N_h$ .

In contrast to the non-stiff case this behaviour does not change so drastically when the noise intensity is increased to  $\sigma = 1$ . In Table 6.6 we still observe a better performance of the BDF2-Maruyama method, although the estimated errors are seemingly affected by the presence of a stronger noise.

To sum up, in our numerical experiments the BDF2-Maruyama method and the two Euler methods performed equally well if the equation is non-stiff and driven by a higher noise intensity. In all other tested scenarios (with stiffness and/or with small noise intensity) the BDF2-Maruyama method is often superior to the two Euler methods in terms of the experimental error. Hence, our observations confirm the results reported earlier in [2].

## 6.2 An example in two dimensions: a toy discretization of an SPDE

Here we consider the two dimensional equation

$$\begin{aligned} dX_1(t) + \frac{1}{2}((1+\lambda)X_1(t) + (1-\lambda)X_2(t)) dt &= (X_1(t) - X_1(t)^3) dt + \sigma X_1(t)^2 dW_1(t), \\ dX_2(t) + \frac{1}{2}((1-\lambda)X_1(t) + (1+\lambda)X_2(t)) dt &= (X_2(t) - X_2(t)^3) dt + \sigma X_2(t)^2 dW_2(t), \end{aligned}$$

for  $t \in (0, T]$ ,  $X(0) = X_0 \in \mathbf{R}^2$  with  $\sigma \geq 0$  and  $\lambda \gg 0$ . We write this equation in the form

$$dX(t) + AX(t)dt = f(X(t))dt + g(X(t))dW(t), \quad t \in (0, T], \quad X(0) = X_0, \quad (6.5)$$

with  $A$  being the positive and symmetric  $2 \times 2$ -matrix

$$A = \frac{1}{\sqrt{2}} \begin{bmatrix} 1 & 1 \\ 1 & -1 \end{bmatrix} \begin{bmatrix} 1 & 0 \\ 0 & \lambda \end{bmatrix} \frac{1}{\sqrt{2}} \begin{bmatrix} 1 & 1 \\ 1 & -1 \end{bmatrix} = \frac{1}{2} \begin{bmatrix} 1+\lambda & 1-\lambda \\ 1-\lambda & 1+\lambda \end{bmatrix},$$

and the non-linearities  $f: \mathbf{R}^2 \rightarrow \mathbf{R}^2$ ,  $g: \mathbf{R}^2 \rightarrow \mathbf{R}^{2 \times 2}$  given by

$$f(x) = \begin{bmatrix} x_1 - x_1^3 \\ x_2 - x_2^3 \end{bmatrix}, \quad g(x) = \sigma \begin{bmatrix} x_1^2 & 0 \\ 0 & x_2^2 \end{bmatrix}, \quad X_0 = (x_1, x_2) \in \mathbf{R}^2.$$

The reason why we are interested in (6.5) is its similarity to the equation obtained when discretizing a stochastic partial differential equation with a Galerkin method. The matrix  $-A$  is a substitute for a discrete Laplacian, which is a symmetric and negative definite matrix. With a Galerkin approximation in  $k$  dimensions the eigenvalues  $\lambda_1 < \lambda_2, \dots, \lambda_{k-1} < \lambda_k$  satisfy that  $\lambda_k \gg 0$  is very large, causing a stiff system. Our matrix  $A$  is chosen to mimic this stiffness. Moreover, our choice of  $f$  is due to its similarity with the nonlinearity of the Allen-Cahn equation. We take the diffusion coefficient to be quadratic in order to demonstrate an example with superlinear growth.

Assumption 2.1 is valid for all  $\lambda \geq 0$  and  $\sigma \in [0, \sqrt{2}/3)$  with  $L = 1$ ,  $q = 3$  and  $\eta = \frac{1}{2\sigma^2}$ . The coercivity condition (2.3) is left to the reader to check and it is in fact it that determines the upper bound for  $\sigma$ . To verify the global monotonicity condition (2.1), we first notice that for  $x, y \in \mathbf{R}^2$ , it holds that

$$\begin{aligned} &(f(x) - f(y), x - y) \\ &= |x - y|^2 - (x_1^3 - y_1^3)(x_1 - y_1) - (x_2^3 - y_2^3)(x_2 - y_2) \\ &= |x - y|^2 - (x_1^2 + x_1y_1 + y_1^2)(x_1 - y_1)^2 - (x_2^2 + x_2y_2 + y_2^2)(x_2 - y_2)^2, \end{aligned}$$

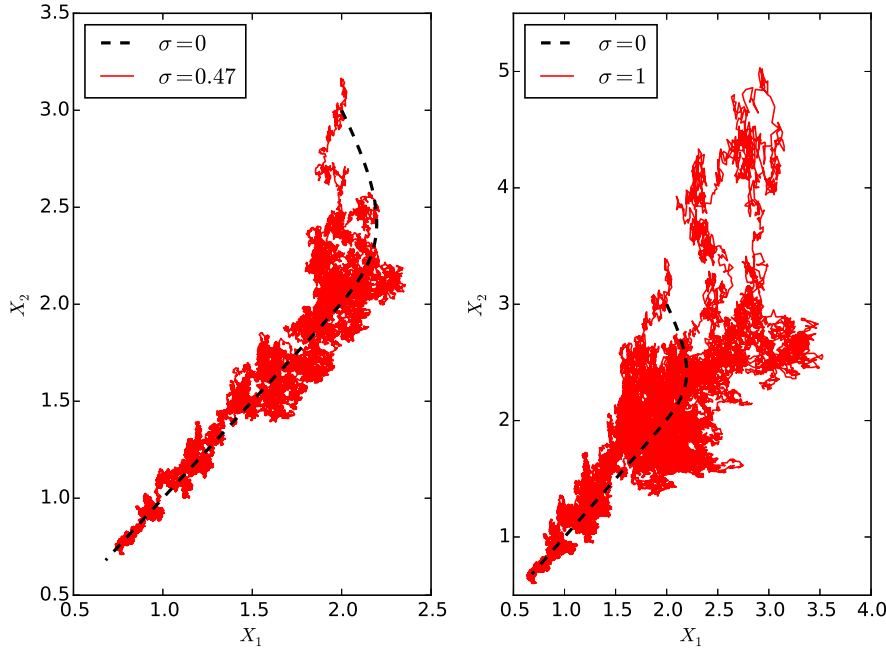


**Fig. 6.1** Sample trajectories computed with BDF2 and  $N = 25 \cdot 2^{12}$  time steps for different noise intensities. The same sample path of the noise is used in both plots.

and that

$$\begin{aligned}
 |g(x) - g(y)|_{\text{HS}}^2 &= \text{Tr}((g(x) - g(y))^*(g(x) - g(y))) \\
 &= \sigma^2 \text{Tr} \left( \begin{bmatrix} (x_1^2 - y_1^2)^2 & \# \\ \# & (x_2^2 - y_2^2)^2 \end{bmatrix} \right) \\
 &= \sigma^2 ((x_1^2 - y_1^2)^2 + (x_2^2 - y_2^2)^2) \\
 &= \sigma^2 ((x_1 - y_1)^2 (x_1 + y_1)^2 + (x_2 - y_2)^2 (x_2 + y_2)^2) \\
 &= \sigma^2 ((x_1 - y_1)^2 (x_1^2 + 2x_1y_1 + y_1^2) + (x_2 - y_2)^2 (x_2^2 + 2x_2y_2 + y_2^2)).
 \end{aligned}$$

Since it also holds that  $-(A(x-y), x-y) \leq 0$  we get for all  $x, y \in \mathbf{R}^2$  that

$$\begin{aligned}
 &(A(x-y) + f(x) - f(y), x-y) + \eta |g(x) - g(y)|_{\text{HS}}^2 \\
 &\leq |x-y|^2 + (\eta\sigma^2 - 1)((x_1^2 + y_1^2)(x_1 - y_1)^2 + (x_2^2 + y_2^2)(x_2 - y_2)^2) \\
 &\quad + (2\eta\sigma^2 - 1)(x_1y_1(x_1 - y_1)^2 + x_2y_2(x_2 - y_2)^2)
 \end{aligned}$$

Under the assumption that  $2\eta\sigma^2 = 1$  we obtain that

$$(A(x-y) + f(x) - f(y), x-y) + \eta |g(x) - g(y)|_{\text{HS}}^2 \leq |x-y|^2, \quad x, y \in \mathbf{R}^2,$$

which proves the global monotonicity for  $L = 1$ .

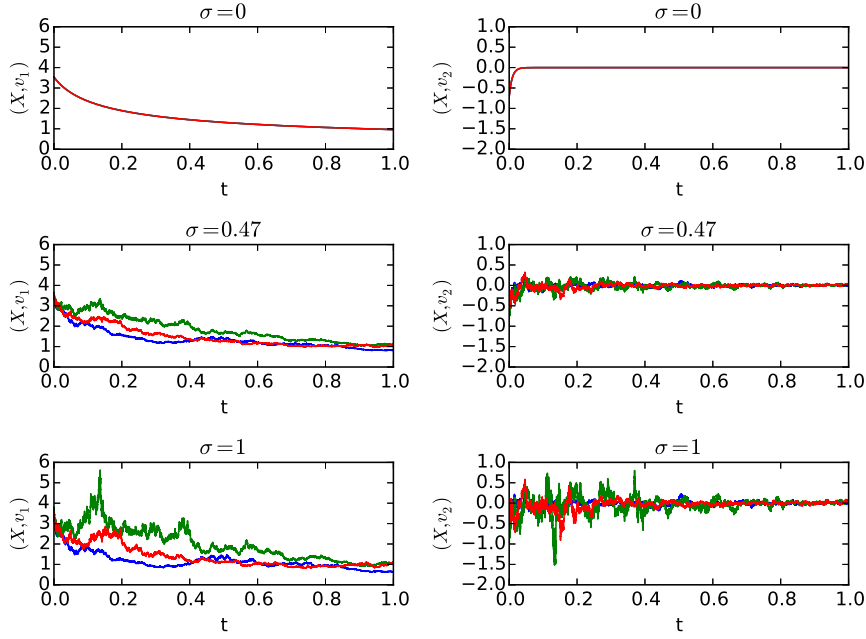


**Fig. 6.2** Projections of several sample paths with different noise intensity onto the eigenvectors  $v_1$  and  $v_2$  of the matrix  $A$ , respectively.

We use the experimental setup of Subsection 6.1. As the equation (6.2) is not explicitly solvable with  $f$  and  $g$  from the present subsection we use  $K = 5$  Newton iterations in each time step to obtain an approximate solution. More precisely, these iterations  $\tilde{X}_h^{j,0}, \dots, \tilde{X}_h^{j,K} = X_h^j$  are given  $\tilde{X}_h^{j,0} = X_h^{j-1}$  and for  $k \in \{1, \dots, K\}$  by  $\tilde{X}_h^{j,k} = \tilde{X}_h^{j,k-1} - (D\Phi_h^j(X_h^{j,k-1}))^{-1} \Phi_h^j(X_h^{j,k-1})$ , where  $\Phi_h^j(x) = x - \beta h(f(x) - Ax) - R_h^j$  and  $D\Phi_h^j$  is the Jacobian. With  $c = \frac{1-\lambda}{2}$  it holds that

$$(D\Phi_h^j(x))^{-1} \Phi_h^j(x) = \frac{1}{(1 - \beta h(c - 3x_1^2))(1 - \beta h(c - 3x_2^2)) - (\beta h c)^2} \times \begin{bmatrix} (1 - \beta h(c - 3x_2^2))(x_1 - \beta h(c(x_1 - x_2) - x_1^3) - R_{h,1}^j) \\ -\beta h c(x_2 - \beta h(c(x_2 - x_1) - x_2^3) - R_{h,2}^j) \\ (1 - \beta h(c - 3x_1^2))(x_2 - \beta h(c(x_2 - x_1) - x_2^3) - R_{h,2}^j) \\ -\beta h c(x_1 - \beta h(c(x_1 - x_2) - x_1^3) - R_{h,1}^j) \end{bmatrix}.$$

This is used for the Newton iterations.

We perform three experiments, all with  $\lambda = 96$ ,  $T = 1$ ,  $X_0 = [2, 3]^t$ , one without noise, i.e.,  $\sigma = 0$ , one with small noise intensity  $\sigma = 0.47$ , which is just below the threshold  $\sqrt{2}/3$  for  $\sigma$ , allowed for the theoretical results to be valid, and one with large noise intensity  $\sigma = 1$  to see how the methods compare outside the allowed parameter regime. Comparing Table 6.7 and 6.8 we observe that the errors differ very

**Table 6.7** Without noise:  $\sigma = 0$ .

$N_h$	EulM		BEM		BDF2	
	error	EOC	error	EOC	error	EOC
25	-	-	0.095559	-	0.062955	-
50	0.512850	-	0.052993	0.85	0.031538	1.00
100	0.036046	3.83	0.028182	0.91	0.013142	1.26
200	0.016245	1.15	0.014630	0.95	0.005002	1.39
400	0.007861	1.05	0.007472	0.97	0.001784	1.49
800	0.003875	1.02	0.003779	0.98	0.000575	1.63
1600	0.001925	1.01	0.001901	0.99	0.000169	1.76
3200	0.000959	1.00	0.000953	1.00	0.000048	1.83

**Table 6.8** Small noise intensity:  $\sigma = 0.47$ .

$N_h$	EulM		BEM		BDF2	
	error	EOC	error	EOC	error	EOC
25	-	-	0.091651	-	0.056638	-
50	-	-	0.051324	0.84	0.029411	0.94
100	0.044452	-	0.027599	0.90	0.012246	1.26
200	0.019432	1.19	0.014429	0.94	0.004621	1.41
400	0.009300	1.06	0.007403	0.96	0.001613	1.52
800	0.004538	1.04	0.003792	0.97	0.000523	1.62
1600	0.002253	1.01	0.001910	0.99	0.000187	1.48
3200	0.001124	1.00	0.000961	0.99	0.000095	0.97

little. This suggests that the noise is negligible for the small noise case and therefore does not effect the dynamics much, but this suggestion is false. This is clear from Figure 6.2, where a typical path is shown and in Figure 6.2, where the same solution path, together with two other solution paths are projected in the directions of the eigenvectors  $v_1 = \frac{1}{\sqrt{2}}[1, 1]^t$  and  $v_2 = \frac{1}{\sqrt{2}}[1, -1]^t$ , corresponding to the eigenvalues 1 and  $\lambda$ , respectively, of the matrix  $A$ . Direction  $v_2$  is the stiff direction. This expresses itself in Figure 6.2 by a strong drift towards zero of  $(X, v_2)$ , while  $(X, v_1)$  is more sensitive to the noise.

For  $N_h = 25$  the CFL-condition  $|1 - \lambda h| < 1$  is not satisfied while for  $N_h \geq 50$  it is. Table 6.7 shows, in the case of no noise, explosion of the Euler-Maruyama method, for the crude refinement levels for which the CFL condition is not satisfied. The backward Euler-Maruyama and BDF2 methods work for all refinement levels and perform better than the Euler-Maruyama method, but only the BDF2 method performs significantly better. For small noise Table 6.8 shows essentially the same errors as for those without noise, only with slightly worse performance for the Euler-Maruyama scheme. Taking into account that the computational effort for the BEM and BDF2-Maruyama schemes are essentially the same our results show the latter to be superior for this problem. Our results confirm the conclusion from the previous subsection that the BDF2-Maruyama scheme performs better for stiff equations with small noise. For  $\sigma = 1$  the Euler-Maruyama scheme explodes for all refinement-levels and BDF2 has lost most of its advantage over BEM. For the crudest step size the error is even higher than for BEM.

**Table 6.9** Large noise intensity:  $\sigma = 1$ .

$N_h$	EulM		BEM		BDF2	
	error	EOC	error	EOC	error	EOC
25	-		0.085359		0.107572	
50	-	-	0.054110	0.66	0.054215	0.99
100	-	-	0.030864	0.81	0.027929	0.96
200	-	-	0.016582	0.89	0.014925	0.90
400	-	-	0.008928	0.89	0.007853	0.93
800	-	-	0.004635	0.95	0.004010	0.97
1600	-	-	0.002372	0.97	0.002135	0.91
3200	-	-	0.001221	0.96	0.001127	0.92

**Acknowledgements** The authors wish to thank Etienne Emmrich for bringing the identity (1.6) to our attention and for informing us about its connection to the BDF2-scheme. Stig Larsson and Chalmers University of Technology are acknowledged for our use of the computational resource Ozzy. This research was carried out in the framework of MATHEON supported by Einstein Foundation Berlin.

## References

1. W.-J. Beyn, E. Isaak, and R. Kruse. Stochastic C-stability and B-consistency of explicit and implicit Euler-type schemes. *J. Sci. Comput.*, 67(3):955–987, 2016.
2. E. Buckwar and R. Winkler. Multistep methods for SDEs and their application to problems with small noise. *SIAM J. Numer. Anal.*, 44(2):779–803 (electronic), 2006.
3. E. Emmrich. Two-step BDF time discretisation of nonlinear evolution problems governed by monotone operators with strongly continuous perturbations. *Comput. Methods Appl. Math.*, 9(1):37–62, 2009.
4. V. Girault and P.-A. Raviart. *Finite element approximation of the Navier-Stokes equations*, volume 749 of *Lecture Notes in Mathematics*. Springer-Verlag, Berlin-New York, 1979.
5. J. Goard and M. Mazur. Stochastic volatility models and the pricing of VIX options. *Math. Finance*, 23(3):439–458, 2013.
6. P. Henry-Labordère. Solvable local and stochastic volatility models: supersymmetric methods in option pricing. *Quant. Finance*, 7(5):525–535, 2007.
7. D. J. Higham, X. Mao, and A. M. Stuart. Strong convergence of Euler-type methods for nonlinear stochastic differential equations. *SIAM J. Numer. Anal.*, 40(3):1041–1063, 2002.
8. Y. Hu. Semi-implicit Euler-Maruyama scheme for stiff stochastic equations. In H. Koerezlioglu, editor, *Stochastic Analysis and Related Topics V: The Silvri Workshop*, volume 38 of *Progr. Probab.*, pages 183–202, Boston, 1996. Birkhauser.
9. M. Hutzenthaler and A. Jentzen. On a perturbation theory and on strong convergence rates for stochastic ordinary and partial differential equations with non-globally monotone coefficients. *Preprint, arXiv:1401.0295v1*, 2014.
10. M. Hutzenthaler and A. Jentzen. Numerical approximations of stochastic differential equations with non-globally Lipschitz continuous coefficients. *Mem. Amer. Math. Soc.*, 236(1112), 2015.
11. M. Hutzenthaler, A. Jentzen, and P. E. Kloeden. Strong and weak divergence in finite time of Euler’s method for stochastic differential equations with non-globally Lipschitz continuous coefficients. *Proc. R. Soc. Lond. Ser. A Math. Phys. Eng. Sci.*, 467(2130):1563–1576, 2011.
12. M. Hutzenthaler, A. Jentzen, and P. E. Kloeden. Strong convergence of an explicit numerical method for SDEs with nonglobally Lipschitz continuous coefficients. *Ann. Appl. Probab.*, 22(4):1611–1641, 2012.
13. P. E. Kloeden and E. Platen. *Numerical Solution of Stochastic Differential Equations*. Springer, Berlin, third edition, 1999.
14. R. Kruse. Characterization of bistability for stochastic multistep methods. *BIT Numer. Math.*, 52(1):109–140, 2012.
15. X. Mao. *Stochastic differential equations and their applications*. Horwood Publishing Series in Mathematics & Applications. Horwood Publishing Limited, Chichester, 1997.

16. X. Mao and L. Szpruch. Strong convergence rates for backward Euler-Maruyama method for nonlinear dissipative-type stochastic differential equations with super-linear diffusion coefficients. *Stochastics*, 85(1):144–171, 2013.
17. G. N. Milstein and M. V. Tretyakov. *Stochastic Numerics for Mathematical Physics*. Scientific Computation. Springer-Verlag, Berlin, 2004.
18. J. M. Ortega and W. C. Rheinboldt. *Iterative solution of nonlinear equations in several variables*, volume 30 of *Classics in Applied Mathematics*. Society for Industrial and Applied Mathematics (SIAM), Philadelphia, PA, 2000. Reprint of the 1970 original.
19. S. Sabanis. Euler approximations with varying coefficients: the case of superlinearly growing diffusion coefficients. *Preprint, arXiv:1308.1796v2*, 2014.
20. A. M. Stuart and A. R. Humphries. *Dynamical Systems and Numerical Analysis*, volume 2 of *Cambridge Monographs on Applied and Computational Mathematics*. Cambridge University Press, Cambridge, 1996.
21. M. V. Tretyakov and Z. Zhang. A fundamental mean-square convergence theorem for SDEs with locally Lipschitz coefficients and its applications. *SIAM J. Numer. Anal.*, 51(6):3135–3162, 2013.